

---

# SKETCHYSGD: RELIABLE STOCHASTIC OPTIMIZATION VIA ROBUST CURVATURE ESTIMATES

---

A PREPRINT

**Zachary Frangella**  
Stanford University  
zfran@stanford.edu

**Pratik Rathore**  
Stanford University  
pratikr@stanford.edu

**Shipu Zhao**  
Cornell University  
sz533@cornell.edu

**Madeleine Udell**  
Stanford University  
udell@stanford.edu

December 5, 2022

## ABSTRACT

We introduce SketchySGD, a stochastic quasi-Newton method that uses sketching to approximate the curvature of the loss function. Quasi-Newton methods are among the most effective algorithms in traditional optimization, where they converge much faster than first-order methods such as SGD. However, for contemporary deep learning, quasi-Newton methods are considered inferior to first-order methods like SGD and Adam owing to higher per-iteration complexity and fragility due to inexact gradients. SketchySGD circumvents these issues by a novel combination of subsampling, randomized low-rank approximation, and dynamic regularization. In the convex case, we show SketchySGD with a fixed stepsize converges to a small ball around the optimum at a faster rate than SGD for ill-conditioned problems. In the non-convex case, SketchySGD converges linearly under two additional assumptions, interpolation and the Polyak-Lojaciewicz condition, the latter of which holds with high probability for wide neural networks. Numerical experiments on image and tabular data demonstrate the improved reliability and speed of SketchySGD for deep learning, compared to standard optimizers such as SGD and Adam and existing quasi-Newton methods.

**Keywords** Stochastic optimization · Quasi-Newton methods · Preconditioning · Randomized numerical linear algebra

## 1 Introduction

Stochastic first-order methods such as SGD and Adam reign supreme for training deep learning models [Davis et al., 2020, Duchi et al., 2011, Johnson and Zhang, 2013, Kingma and Ba, 2014, Sun, 2019] due to their robustness to nonconvex landscapes and efficient iterations. However, SGD and its variants alone typically do not suffice to ensure successful training. Indeed, in order to successfully reach a point with good generalization properties extensive hyperparameter tuning, e.g., adjusting learning rates, momentum, and decay schedules, is required. As described by Yao et al. [2021], "...one has to *babysit* the optimizer to make sure that training converges to an *acceptable* training loss..."

The need to carefully tune the optimizer can be expensive in terms of human capital, computational costs, and environmental impact. Manual tuning of the optimizer is costly in terms of man-hours and computational resources, as one may need to train with several different learning rates, while repeatedly checking progress, to find a model that yields good performance. In fact, "the computational cost of [AI] research is increasing exponentially, at a pace that far exceeds Moore's Law" [Schwartz et al., 2020], and this computational burden is compounded further by having to train multiple models with different hyperparameters. Additionally, heavy computational cost directly correlates with increased environmental burden, as large-scale deep learning models come with heavy carbon footprints [Schwartz et al., 2020].

In convex optimization, second-order optimizers based on the Hessian, such as Newton's method and quasi-Newton methods converge at super-linear rates under mild assumptions, making them much faster than first-order methods [Nocedal and Wright, 1999, Boyd and Vandenberghe, 2004]. Given the success of second-order methods in convex settings, we would hope that these methods outperform first-order methods such as SGD in deep learning. Alas, second

order methods come with three significant limitations that forbid their use in deep learning. First, the per-iteration cost of Newton and quasi-Newton methods is much higher than gradient based methods. These costs are high but surmountable with an indirect solver like conjugate gradients (CG) with efficient (backprop-based) Hessian-vector products; we elaborate in Section 2.1. Second, these methods are not robust to stochastic gradients in theory and in practice their performance is unreliable; see experiments in Section 4. Third, although these methods can drive the training loss to a relatively small value in a few iterations, they often stall at a saddle point that does not generalize well to the test dataset [Dauphin et al., 2014]. The major innovation in this paper is the use of sketching to produce a new robust stochastic quasi-Newton framework we call SketchySGD. We show that SketchySGD gives comparable performance to popular optimizers such as SGD and Adam in the deep learning setting, while having robust performance with respect to the learning rate. In addition, we prove that SketchySGD converges at a faster rate than SGD in the convex setting, and is robust to ill-conditioning.

## 1.1 SketchySGD

SketchySGD solves empirical risk minimization problems of the form

$$\text{minimize}_{w \in \mathbb{R}^p} f(w) := \frac{1}{n} \sum_{i=1}^n f_i(w)$$

given access to a subgradient oracle (computed, e.g., with automatic differentiation (AD)) for each  $f_i$ . Given iterate  $w_k$  at iteration  $k$ , SketchySGD samples two independent batches  $S_k$  and  $B_k \subseteq [n]$  of data and computes a stochastic gradient  $g_{B_k}(w_k)$  and a randomized low-rank approximation  $\hat{H}_{S_k}$  to the subsampled Hessian  $H_{S_k}(w_k)$ . The approximate Hessian may be constructed from a sketch of the Hessian computed via AD as detailed in Section 2 at a cost only a constant factor larger than computing a stochastic gradient. SketchySGD forms a regularized stochastic approximation to the Hessian ( $\hat{H}_{S_k} + \rho_k I$ ) and updates the parameters as

$$w_{k+1} = w_k - \eta_k (\hat{H}_{S_k} + \rho_k I)^{-1} g_{B_k}(w_k), \tag{1}$$

where  $\eta_k$  is the learning rate and  $\rho_k > 0$  is a regularization parameter. The SketchySGD update may be viewed as a preconditioned stochastic gradient step with Levenberg-Marquardt regularization [Levenberg, 1944, Marquardt, 1963] or as a stochastic quasi-Newton method with inexact gradients.

### Contributions.

1. We develop a new robust stochastic quasi-Newton algorithm that is fast and generalizes well by accessing only a subsampled Hessian and stochastic gradient.
2. In the convex case, we show that SketchySGD converges to the optimum at a faster rate than SGD for ill-conditioned problems. In the non-convex case, we show that SketchySGD converges linearly to the optimum for wide neural networks under the Polyak-Lojaciwicz condition and interpolation.
3. We present logistic regression experiments showing that SketchySGD with a theoretically-motivated learning rate can match or outperform SGD, Adam, SAGA, SVRG, and L-BFGS. These experiments corroborate our theory that SketchySGD converges at a faster rate than SGD.
4. We present deep learning experiments showing that SketchySGD reliably yields models that generalize well across a variety of learning rates on both tabular and image tasks, while SGD and Adam often yield poor performance without careful selection of the learning rate.
5. We compare SketchySGD to several quasi-Newton methods for deep learning. We find SketchySGD yields comparable or better performance, is the most robust, and is either faster or comparable to its competitors in terms of runtime.

**Outline.** Section 2 describes the SketchySGD algorithm in detail, explaining how to compute  $\hat{H}_{S_k}$  and the update in (1) efficiently. Section 2.1 surveys previous work on stochastic quasi-Newton methods, particularly in the context of machine learning. Section 3 establishes convergence of SketchySGD in both convex and non-convex settings. Section 4 provides numerical experiments showing the superiority of SketchySGD relative to competing optimizers.

## 2 SketchySGD

**Notation.** Throughout the paper  $B_k$  and  $S_k$  denote subsets of  $\{1, \dots, n\}$  that are sampled independently and uniformly without replacement. The corresponding stochastic gradient and minibatch Hessian are given by

$$g_{B_k}(w) = \frac{1}{b_{g_k}} \sum_{i \in B_k} g_i(w),$$

$$H_{S_k}(w) = \frac{1}{b_{h_k}} \sum_{i \in S_k} \nabla^2 f_i(w),$$

where  $b_{g_k} = |B_k|$ ,  $b_{h_k} = |S_k|$ . For shorthand we often omit the dependence upon  $w$  and simply write  $g_{B_k}$  and  $H_{S_k}$ . We also define  $H(w)$  as the Hessian of the objective  $f$  at  $w$ , and we set  $M(w) = \max_{1 \leq i \leq n} \|\nabla^2 f_i(w)\|$ . Given any  $\tau > 0$ , we use the notation  $H_{S_k}^\tau$  to denote  $H_{S_k} + \tau I$ . We abbreviate positive-semidefinite as psd. We denote the Loewner order on the convex cone of psd matrices by  $\preceq$ , where  $A \preceq B$  means  $B - A$  is psd. Given a psd matrix  $A \in \mathbb{R}^{p \times p}$ , we enumerate its eigenvalues in descending order,  $\lambda_1(A) \geq \lambda_2(A) \geq \dots \geq \lambda_p(A)$ . Finally given a psd matrix  $A$  and  $\tau > 0$  we define the effective dimension by  $d_{\text{eff}}(\tau) = \text{tr}(A(A + \tau I)^{-1})$ , which provides a smoothed measure of the eigenvalues greater than or equal to  $\tau$ .

**Hessian vector product via autodiff.** SketchySGD relies on one main computational primitive, a (minibatch) Hessian vector product (hvp), to compute a low-rank approximation of the (minibatch) Hessian. An hvp can be computed by automatic differentiation (AD); it requires roughly twice the computation of one (minibatch) gradient, or  $O(p)$  with a constant batch size. In contrast, explicitly instantiating a Hessian entails a heavy  $O(p^2)$  storage and  $O(np^2)$  computational cost.

Let  $g_{S_k} \in \mathbb{R}^p$  denote the gradient with respect to the sampled minibatch  $S_k \subseteq [n]$ , and let  $\varphi \in \mathbb{R}^p$  be a vector. Then calculus yields an expression for the minibatch hvp  $H_{S_k} \varphi$  as the gradient of  $g_{S_k}^\top \varphi$ :

$$\frac{\partial}{\partial w} (g_{S_k}^\top \varphi) = g_{S_k}^\top \frac{\partial \varphi}{\partial w} + \frac{\partial g_{S_k}}{\partial w} \varphi = 0 + H_{S_k} \varphi = H_{S_k} \varphi. \quad (2)$$

That is, given the gradient  $g_{S_k}$ , the hvp  $H_{S_k} \varphi$  can be computed by AD on the scalar function  $g_{S_k}^\top \varphi$  with respect to  $w$ . This technique has been used in several recent papers [Ghorbani et al., 2019, Yao et al., 2020, 2021] that use Hessian information, and goes back to Pearlmutter [1994].

**Randomized low-rank approximation.** The hvp primitive allows for efficient randomized low-rank approximation to the minibatch Hessian by sketching. Sketching reduces the cost of fundamental numerical linear algebra operations without much loss in accuracy [Woodruff, 2014, Martinsson and Tropp, 2020] by computing the quantity of interest from a *sketch*, or randomized linear image, of a matrix. In particular, sketching enables efficient computation of a near-optimal low-rank approximation to  $H_{S_k}$  [Halko et al., 2011, Cohen et al., 2015, Tropp et al., 2017a].

SketchySGD computes a sketch of the subsampled Hessian using hvps and returns a randomized low-rank approximation  $\hat{H}_{S_k}$  of  $H_{S_k}$  in the form of an eigendecomposition  $\hat{V} \hat{\Lambda} \hat{V}^\top$ , where  $\hat{V} \in \mathbb{R}^{p \times r}$  and  $\hat{\Lambda} \in \mathbb{R}^{r \times r}$ . Many algorithms are available to construct a low-rank approximation from the sketch, including the randomized SVD [Halko et al., 2011]. In this paper, we use the randomized Nyström approximation, following the stable implementation in Tropp et al. [2017b].

When the loss is convex,  $H_{S_k}$  is symmetric psd; otherwise,  $H_{S_k}$  is not guaranteed to be psd. To handle non-convex problems for which the subsampled Hessian may not be psd, SketchySGD uses *dynamic regularization* to ensure all eigenvalues of the approximation are nonnegative. The resulting algorithm appears in the supplement as `RandPDLowRankApprox`.

**Algorithm 1** SketchySGD

---

**input:** initialization  $w_0$ , ranks  $\{r_j\}$ , regularization  $\{\rho_k\}$ , learning rates  $\{\eta_k\}$ , Hessian update frequency  $u$

**repeat**

Sample independent batches  $S_k$  and  $B_k$

Compute stochastic gradient  $g_{B_k}(w_k)$  ▷ via AD

**if**  $k \equiv 0 \pmod{u}$  **then**

$\Phi = \frac{1}{\sqrt{p}} \text{randn}(p, r_{k/u})$  ▷ Gaussian test matrix

Compute sketch  $Y = H_{S_k}(w_k)\Phi$  ▷  $r$  hvps

$[\hat{V}, \hat{\Lambda}] = \text{RandPDLowRankApprox}(Y, \Phi, r)$

Compute  $v_k = (\hat{H}_{S_k} + \rho_k I)^{-1} g_{B_k}(w_k)$  via (3)

$w_{k+1} = w_k - \eta_k v_k$  ▷ Update parameters

**until** convergence

---

**SketchySGD.** As shown in Algorithm 1, the SketchySGD method uses a low-rank approximation to a minibatch Hessian to perform a stochastic quasi-Newton update with the minibatch gradient. SketchySGD reestimates the approximation to the minibatch Hessian at frequency  $u$  to ensure fast convergence; empirically, reestimating every epoch (i.e., one pass through the training data) or two suffices. In practice, a constant rank  $r$  between 50 and 100 works well. While several hyperparameters appear in the algorithm, including the sequence of ranks  $\{r_j\}$ , regularizations  $\{\rho_k\}$ , and learning rates  $\{\eta_k\}$ , one major benefit of SketchySGD is robustness to these choices. We present default values, which work well and robustly, in the supplement.

Given the rank- $r$  approximation  $\hat{H}_{S_k} = \hat{V}\hat{\Lambda}\hat{V}^\top$  to the minibatch Hessian  $H_{S_k}$ , the main cost of SketchySGD relative to standard SGD is computing the search direction  $v_k = (\hat{H}_{S_k} + \rho_k I)^{-1} g_{B_k}$ . This (parallelizable) computation requires  $O(pr)$  flops, by the Woodbury formula [Higham, 2002]:

$$v_k = \hat{V} \left( \hat{\Lambda} + \rho_k I \right)^{-1} \hat{V}^\top g_{B_k} + \frac{1}{\rho_k} (g_{B_k} - \hat{V} \hat{V}^\top g_{B_k}). \quad (3)$$

**And it’s fast!** The cost of a fresh low-rank Hessian approximation is  $O((b_{h_k} + r^2)p)$ . Given this approximation, the cost of each iteration (i.e., quasi-Newton step) is only  $O((b_{g_k} + r)p)$ . With a typical batch size of 256 or 512 for SGD and rank  $r = 100$  for SketchySGD, the complexity per iteration is only about 20–40% larger than standard SGD. With weight-sharing, the time to compute a backprop step increases relative to the number of parameters, which makes the additional matrix computations required to implement SketchySGD even cheaper in comparison.

## 2.1 Comparison to previous work

Many authors have sought to scale Newton’s method and its variants to large-scale machine learning tasks. Classical approaches include BFGS, its low-memory variant L-BFGS, and inexact Newton methods, where the sub-problem is solved approximately [Broyden, 1970, Liu and Nocedal, 1989, Dembo et al., 1982]. Given a function and gradient oracle, BFGS and L-BFGS yield satisfactory solutions to most optimization problems. However, for very large-scale problems, the cost of computing an exact gradient or function evaluation at each iteration is too large; hence methods for these problems must work with sampled function values and stochastic gradients.

*Stochastic quasi-Newton methods* address both problems by taking a generalized Newton step using a stochastic approximation to the Hessian (and, sometimes, to the gradient as well). Stochastic quasi-Newton methods that use exact gradients with a stochastic Hessian approximation constructed via sketching or subsampling include Byrd et al. [2011], Erdogdu and Montanari [2015], Pilanci and Wainwright [2017], Gower et al. [2019]. Others, such as Roosta-Khorasani and Mahoney [2019], Bollapragada et al. [2019], Meng et al. [2020], can handle stochastic approximations to both the gradient and Hessian. Among this work, our convergence analysis in the non-convex case is inspired by Meng et al. [2020], who identify the key role of interpolation in establishing convergence without requiring increasingly accurate approximations to the gradient.

In recent years there has been a flurry of work focusing on quasi-Newton methods for deep learning. Grosse and Martens [2016] uses a Kronecker-factored approximation to the Fisher information matrix, which leads to a scalable approximate natural gradient method called K-FAC. Yang et al. [2020] develops another approximate natural gradient method called the Sketchy Empirical Natural Gradient (SENG) method. The authors find SENG delivers better performance than K-FAC and first-order methods such as Adam. K-FAC and SENG are not the only methods that approximate the natural gradient; others include Roux et al. [2007], Yang et al. [2021a]. Gupta et al. [2018] introduces

Shampoo, which preconditions stochastic tensor iterations using the second moments of accumulated gradients. Taking a more classical approach, Goldfarb et al. [2020], Yang et al. [2021b] design versions of L-BFGS tailored to neural networks. Another recent method is AdaHessian [Yao et al., 2021]. AdaHessian reduces the complexity of Newton’s method by replacing the inverse Hessian with a randomized diagonal approximation. All of these methods have been observed to improve performance relative to standard optimizers such as SGD and Adam, and are comparable in cost, excluding K-FAC, and Shampoo, which are much slower than SGD, Adam, and our method, SketchySGD.

SketchySGD improves on these previous stochastic quasi-Newton methods and generalizes many of them. In particular, subsampled Newton methods [Roosta-Khorasani and Mahoney, 2019, Bollapragada et al., 2019, Meng et al., 2020] may be viewed as a special case of SketchySGD that uses the true minibatch Hessian instead of its low-rank approximation. We recover the method of Erdogdu and Montanari [2015] by using exact gradients and a regularized exact low-rank approximation to the subsampled Hessian. SketchySGD is theoretically much faster than or comparable to prior work on stochastic quasi-Newton methods. Table 1 compares the complexity per iteration of SketchySGD to prior methods that work in the deep learning setting, assuming the Hessian approximation of SketchySGD is updated once per epoch. Although SketchySGD’s theoretical complexity is larger than AdaHessian’s, our method generally requires fewer hvps, since SketchySGD computes  $r$  hvps per epoch, while AdaHessian computes  $O(N)$  hvps per epoch, where  $N$  is the number of minibatches. For large-scale problems,  $N$  is typically much larger than  $r = 100$ . In our experiments, we see that SketchySGD is significantly cheaper than all previous stochastic (quasi-)Newton methods and is comparable to SGD and Adam.

Table 1: Per-iteration Complexity of Stochastic Quasi-Newton Methods

Method	Iteration Complexity	References
Subsampled Newton-CG (inexact gradients)	$\tilde{O}\left(\left(\sqrt{\kappa(H_{S_k})}b_{h_k} + b_{g_k}\right)p\right)$	Roosta-Khorasani and Mahoney [2019], Bollapragada et al. [2019], Meng et al. [2020]
AdaHessian	$O(b_{g_k}p)$	Yao et al. [2021]
SENG	$O((b_{g_k} + b_{h_k}^2)p)$	Yang et al. [2020]
SketchySGD	$O((b_{g_k} + r)p)$	This paper

### 3 Theory

We now prove convergence of SketchySGD both when  $f$  is convex and when  $f$  is non-convex but interpolating and satisfies the Polyak-Lojaciewicz (PL) condition. We begin with an assumption needed throughout.

**Assumption 1** (Differentiability and smoothness). *The function  $f$  is twice differentiable and  $L$ -smooth. Further, each  $f_i$  is  $L_i$ -smooth with  $L_i \leq L_{\max}$  for every  $i = 1, \dots, n$ .*

#### 3.1 Convex case

Our analysis of the convex case requires the bounded iterates, strong convexity, and the notions of relative smoothness and relative convexity.

**Assumption 2** (Bounded iterates). *The iterates of Algorithm 1 lie in a compact set  $\mathcal{X}$  containing  $w_*$ .*

**Assumption 3** (Strong convexity). *The function  $f$  is  $\mu$ -strongly convex for some  $\mu > 0$ .*

**Assumption 4** (Relative smoothness and relative convexity). *There exist constants  $\hat{L} \geq \hat{\mu} > 0$  such that for all  $w, w' \in \mathcal{X}$ :*

$$f(w') \leq f(w) + \langle g(w), w' - w \rangle + \frac{\hat{L}}{2} \|w' - w\|_{H(w)}^2, \quad (4)$$

$$f(w') \geq f(w) + \langle g(w), w' - w \rangle + \frac{\hat{\mu}}{2} \|w' - w\|_{H(w)}^2. \quad (5)$$

Relative smoothness and relative convexity were introduced in Gower et al. [2019]. These assumptions are weaker than assuming  $f$  is  $L$ -smooth and  $\mu$ -strongly convex. Indeed, it is easy to show that if  $f$  is  $L$ -smooth and  $\mu$ -strongly convex then (4) and (5) hold, see Gower et al. [2019] for details. More importantly, (4) and (5) hold with non-vacuous values of  $\hat{L}$  and  $\hat{\mu}$ . In the case of least-squares  $\hat{L} = \hat{\mu} = 1$ , and for generalized linear models  $\hat{L}$  and  $\hat{\mu}$  are  $O(1)$  and independent

of the condition number  $\kappa = L/\mu$  [Gower et al., 2019]. Thus, for many popular machine learning problems the *relative condition number*  $\hat{\kappa} = \hat{L}/\hat{\mu}$  is a constant independent of the conditioning of the data.

The worst case  $(r + 1)$ th eigenvalue of the Hessian plays an important role in our convergence result.

**Definition 1.** Fix  $1 \leq r \leq p$ , and set

$$\lambda_{r+1}^* = \sup_{w \in \mathcal{X}} \lambda_{r+1}(H(w)).$$

Observe  $\lambda_{r+1}^* \leq L$  and is often significantly smaller. For the least-squares loss,  $\lambda_{r+1}^* = \lambda_{r+1}(H)$  and  $L = \lambda_1(H)$ . As most machine learning data matrices exhibit polynomial or exponential spectral decay, [Zhao et al., 2022, Derezhinski et al., 2020] we generally have  $\lambda_{r+1}(H) \ll \lambda_1(H)$  and hence  $\lambda_{r+1}^* \ll L$ .

**Theorem 5** (SketchySGD convex convergence – informal). *Instate Assumptions 1, 2, 3, and 4. Run Algorithm 1 with batch sizes  $b_g, b_{h_k} = \tilde{O}\left(\frac{M(w_k)}{\lambda_{r+1}^*}\right)$ , stepsize  $\eta = O(\hat{\kappa}^{-1})$ , fixed regularization  $\rho = \lambda_{r+1}^*$ , and at each iteration constructing the randomized Nyström approximation with rank  $r_k = \tilde{O}(\text{d}_{\text{eff}}(\zeta \lambda_{r+1}^*))$  where  $r > 0$  is fixed. Then with high probability, for sufficiently small  $\epsilon$ ,*

$$\mathbb{E}[f(w_T)] - f(w_*) \leq \epsilon$$

after  $T = O\left(\frac{\lambda_{r+1}^* \hat{\kappa} \log(\frac{1}{\epsilon})}{\mu \epsilon}\right)$  iterations.

**Remark 1.** The formal version of Theorem 5 appears in the supplement.

We have the following corollary that gives the improvement ratio of SketchySGD relative to SGD.

**Corollary 1.** *Let  $T_{\text{SketchySGD}}$  denote the iteration complexity of SketchySGD from Theorem 5 and  $T_{\text{SGD}}$  denote the iteration complexity of SGD given from Theorem 4.6 in Gower et al. [2021]. Then*

$$\frac{T_{\text{SGD}}}{T_{\text{SketchySGD}}} \geq \frac{\hat{\mu}}{\hat{\kappa}} \frac{L}{30\lambda_{r+1}^*}.$$

In particular, in the case of the least-squares loss we have

$$\frac{T_{\text{SGD}}}{T_{\text{SketchySGD}}} \geq \frac{L}{30\lambda_{r+1}^*} = \frac{\lambda_1(H)}{30\lambda_{r+1}(H)}.$$

For ill-conditioned problems, we expect the ratio  $L/\lambda_{r+1}^*$  to satisfy  $L/\lambda_{r+1}^* \gg 1$ , in which case SketchySGD will be significantly faster than SGD. This is exactly the setting where we would expect SketchySGD to be useful. Indeed, if the problem is very well-conditioned than SGD is sufficient as there is no need to precondition.

### 3.2 SketchySGD converges for wide neural networks

In this subsection, we show SketchySGD converges for wide neural networks. The analysis requires two more assumptions.

**Assumption 6** (PL condition). *Function  $f$  satisfies the PL inequality if*

$$\frac{1}{2}\|g(w)\|^2 \geq \theta(f(w) - f(w_*)), \forall w.$$

A function that is  $L$ -smooth and  $\theta$ -PL always has  $\theta \leq L$ ; see more details in the supplement.

**Assumption 7** (Interpolation). *Any optimal classifier  $w_* \in \mathcal{W}_*$  interpolates the training set:  $\|g_i(w_*)\| = 0$  for each  $i \in \{1, \dots, n\}$ .*

In the supplement, we show that under Assumptions 6 and 7 SketchySGD converges linearly to the optimum. We then invoke existing theory that guarantees interpolation and the PL condition for wide neural nets to show that SketchySGD converges linearly on wide neural networks.

The PL condition and interpolation are common assumptions in convergence analysis for non-convex optimization, especially for deep learning [Vaswani et al., 2019a, Gower et al., 2021]. Liu et al. [2022] showed that sufficiently wide neural networks satisfy the PL condition. This result holds for multilayer perceptrons (MLPs) as well as more sophisticated architectures such as ConvNets and ResNets. Further, apriori, over-parameterized neural networks are believed to interpolate the training dataset [Vaswani et al., 2019b,a, Meng et al., 2020, Ma et al., 2018], and it is now standard practice for many problems to train until the model interpolates the training set (or longer) [Belkin, 2021].

Using the results in Liu et al. [2022], we establish convergence theory for SketchySGD on wide neural networks. As an example, we state the following theorem for MLPs. As in Liu et al. [2022], define a scalar-valued  $L$ -layer MLP  $F_{\text{NN}}(w; x)$  with weights  $w \in \mathbb{R}^p$ , width  $m^\ell$  for each layer  $\ell \in \{1, \dots, L\}$ , and input  $x \in \mathbb{R}^d$ . Given a dataset  $\{x_1, \dots, x_n\}$ , stack the output of the MLP at each data point into a vector and write the result as a function of the parameters  $w$  as  $\mathcal{F}_{\text{NN}}(w) \in \mathbb{R}^n$ . Define the *tangent kernel* of  $F_{\text{NN}}$  at  $w$  as  $K(w) = \mathcal{D}\mathcal{F}_{\text{NN}}(w)\mathcal{D}\mathcal{F}_{\text{NN}}(w)^T$ , where  $\mathcal{D}\mathcal{F}_{\text{NN}}(w)$  denotes the Jacobian.

**Theorem 8** (SketchySGD converges on wide MLPs). *Consider an MLP  $F_{\text{NN}}(w, x)$  with weights  $w_0$  initialized according to a standard Gaussian distribution and fit on a dataset of size  $n$  using the square-loss  $f(w) = \|\mathcal{F}_{\text{NN}}(w) - y\|^2$ . Suppose the last layer activations  $\sigma^{L+1}$  satisfy  $|\nabla \sigma^{L+1}| \geq \gamma > 0$ ,  $K(w_0)$  has positive smallest eigenvalue  $\lambda_0$ , and at each layer  $\ell = 1, \dots, L$  the width  $m^\ell$  of the network satisfies*

$$m^\ell = \tilde{\Omega} \left( \frac{nR^{6L+2}}{(\lambda_0 - \theta\gamma^{-2})^2} \right)$$

for any  $\theta \in (0, \lambda_0\gamma^2)$ . Instate Assumptions 1, 6, 7, 18. Run SketchySGD from any initialization  $w_0 \in \mathbb{R}^p$ , with constant batch sizes for  $B_k$  and  $S_k$ , and appropriate step size and regularization sequences. Then with high probability SketchySGD converges linearly to a global optimizer  $w_*$  within the ball  $B(w_0, R)$  for some  $R > 0$ .

**Remark 2.** Theorem 8 pertains only to the square loss function. Convergence for other popular loss functions can be established using ideas from Scaman et al. [2022].

## 4 Numerical experiments

In this section, we evaluate the performance of SketchySGD through four groups of experiments. The first group of experiments is in the logistic regression setting (Section 4.1), where we compare the performance of SketchySGD to SGD, SVRG [Johnson and Zhang, 2013], SAGA [Defazio et al., 2014], Adam [Kingma and Ba, 2014], and L-BFGS [Liu and Nocedal, 1989]. The second, third, and fourth groups of experiments are in the deep learning setting. The second and third groups train classifiers on tabular data (Section 4.2.1) and image data (Section 4.2.2), respectively. These experiments compare SketchySGD with Adam and SGD to show its effectiveness and reliability in practice compared to commonly used methods across different types of tasks; the image classification experiments also add AdamW [Loshchilov and Hutter, 2019] as a point of comparison. The fourth group of experiments (Section 4.2.3) compares SketchySGD to other quasi-Newton methods including AdaHessian [Yao et al., 2021], Shampoo [Gupta et al., 2018], K-FAC [Grosse and Martens, 2016], and SENG [Yang et al., 2020] to show the significant speedup and robustness SketchySGD offers compared to other quasi-Newton methods.

Additional details appear in the appendix and code to reproduce our experiments is forthcoming on GitHub.

### 4.1 Logistic regression

In the logistic regression setting, we initialize SGD, SVRG, and Adam with a fixed learning rate  $\eta$ . For SVRG we update the variance-reduced gradient at every epoch. The learning rate for L-BFGS and SAGA are automatically selected by scikit-learn, and the learning rate for SketchySGD is given by  $1/(1 + 100\hat{\lambda}_r)^{-1}$ , where  $\hat{\lambda}_r$  is the  $r$ th eigenvalue of the current approximation  $\hat{H}$  to the subsampled Hessian. We update the approximation  $\hat{H}$  every epoch. We run SketchySGD with regularization  $\rho = 10^{-3}$  and rank  $r = 50$ . We also use a L2-regularization of  $10^{-2}/n_{\text{tr}}$ , where  $n_{\text{tr}}$  is the number of training samples.

We train logistic regression classifiers on the IJCNN [Prokhorov], News20 [Lang, 1995], and RCV1 [Lewis et al., 2004] datasets. For IJCNN, we apply a random features transformation corresponding to the Gaussian kernel [Rahimi and Recht, 2007]. We run SGD, SVRG, and Adam with learning rates varying from 0.001 to 1, and select the run with the highest peak test accuracy (the highest test accuracy attained across all epochs and across all learning rates).

The results are presented in Figure 1. For all four tasks, we observe that SketchySGD converges much faster than SGD to a model with good test accuracy. This improved convergence is an empirical confirmation that SketchySGD converges at a faster rate than SGD for convex problems, as shown in Theorem 5. In addition, SketchySGD outperforms SVRG and L-BFGS and performs comparably to Adam and SAGA on all tasks.

### 4.2 Deep learning

In the deep learning setting, we initialize each optimizer with a learning rate  $\eta$ , which is decreased by a factor of 10 at a fixed number of epochs (80, 120, and 160 for image tasks, 10 and 20 for tabular tasks). We use a weight decay of

<sup>1</sup>This is a theoretically-motivated choice; see the supplement for details.

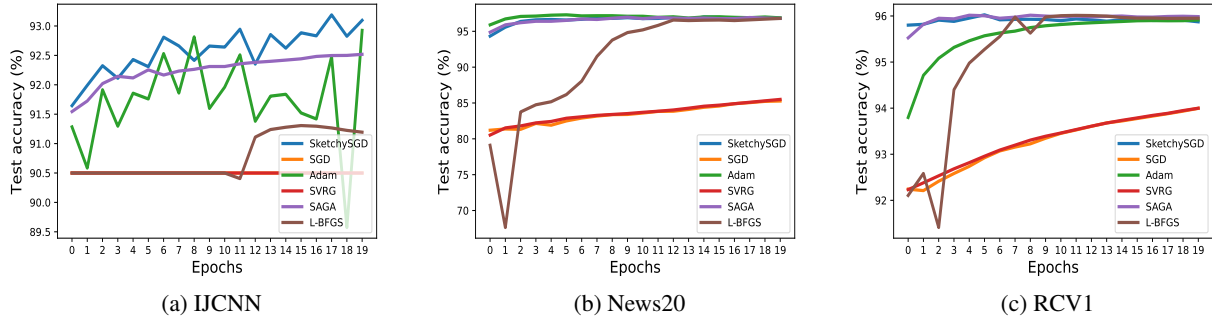


Figure 1: Performance of SketchySGD, SGD, Adam, SVRG, SAGA, and L-BFGS in the logistic regression setting. The test accuracy curves for SGD, Adam, and SVRG are selected according to the peak test accuracy.

$5 \cdot 10^{-4}$  for all optimizers. We run SketchySGD with regularization  $\rho = \eta$  that decays with the learning rate, and use rank  $r = 100$  for all the tasks. (These parameters seem not to require tuning: a remarkable testament to the reliability of SketchySGD!) We also update the Hessian approximation  $\hat{H}$  every two epochs. All the methods are implemented using PyTorch, which uses a BSD licence [Paszke et al., 2019].

#### 4.2.1 Tabular data

The goal of the tabular tasks is to train an MLP to classify test instances in the Higgs [Baldi et al., 2014], MiniBooNE [min], and Volkert [vol] datasets. To assess the robustness of SketchySGD, SGD, and Adam, we train the MLP models with learning rates varying from 0.0001 to 3 and plot the test accuracy curves to visualize the robustness of each optimizer to this hyperparameter.

The results are presented in Figure 2. In each subfigure, the solid lines indicate the median test accuracy curve for each method (over each learning rate), and the 75% *quantile interval* is represented by the shaded area and bounded by the 12.5% and 87.5% quantiles. The 75% quantile interval of SketchySGD is much narrower than that of Adam and SGD: that is, SketchySGD is much more robust to different learning rate settings. Second, for all the tasks, SketchySGD matches or exceeds the peak test accuracy reached by SGD and Adam, as shown in Table 2.

Table 2: Peak Test Accuracy for Tabular Tasks

Accuracy \ Method	SketchySGD	SGD	Adam
Higgs (%)	75.45	75.47	75.28
MiniBooNE (%)	93.40	92.08	92.90
Volkert (%)	65.37	58.97	64.24

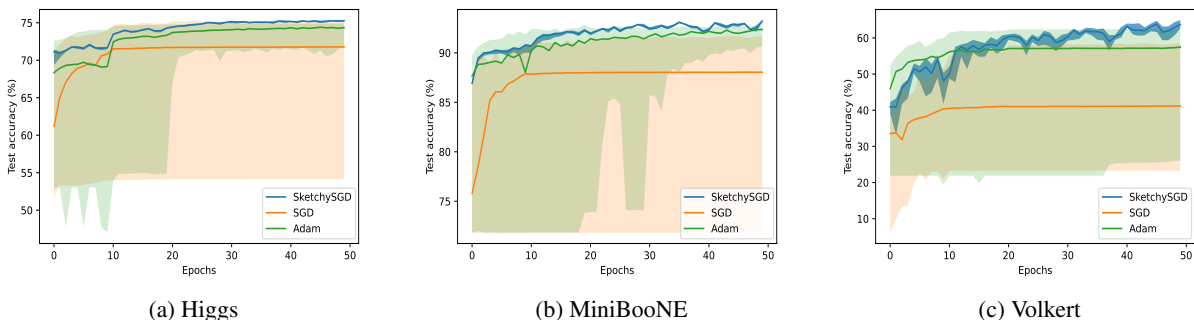


Figure 2: SketchySGD converges robustly and nearly as fast or faster than SGD and Adam on tabular data tasks. The solid line indicates the median of test accuracy among different learning rate settings, and the shaded area represents the 75% quantile interval.

Table 3: Peak Test Accuracy for Image Classification Tasks

Accuracy \ Method	SketchySGD	SGD	Adam	AdamW
CIFAR-10 (%)	91.90	92.51	91.31	92.06
SVHN (%)	95.97	96.61	96.12	96.58

#### 4.2.2 Image classification

Our image classification tasks train ResNet20 on CIFAR-10 and ResNet32 on SVHN [Krizhevsky et al., 2009, Netzer et al., 2011, He et al., 2016]. Again, we train the ResNet models with different learning rates sampled from 0.0001 to 3 and report the median and 75% quantile interval of the test accuracy curves.

Figure 3 and Table 3 present the results using the same conventions as in Section 4.2.1. SketchySGD converges nearly as fast as SGD, Adam, and AdamW and is more robust to different learning rate settings. SketchySGD reaches peak test accuracy comparable to SGD, Adam, and AdamW.

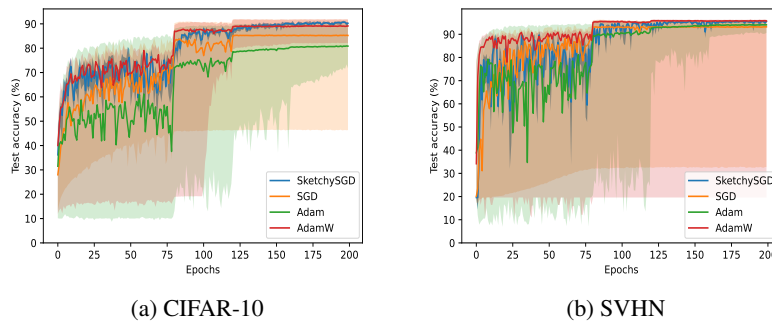


Figure 3: SketchySGD converges robustly and nearly as fast as SGD, Adam, and AdamW on image classification tasks. The solid line indicates the median of test accuracy among different learning rate settings, and the shaded area represents the 75% quantile interval.

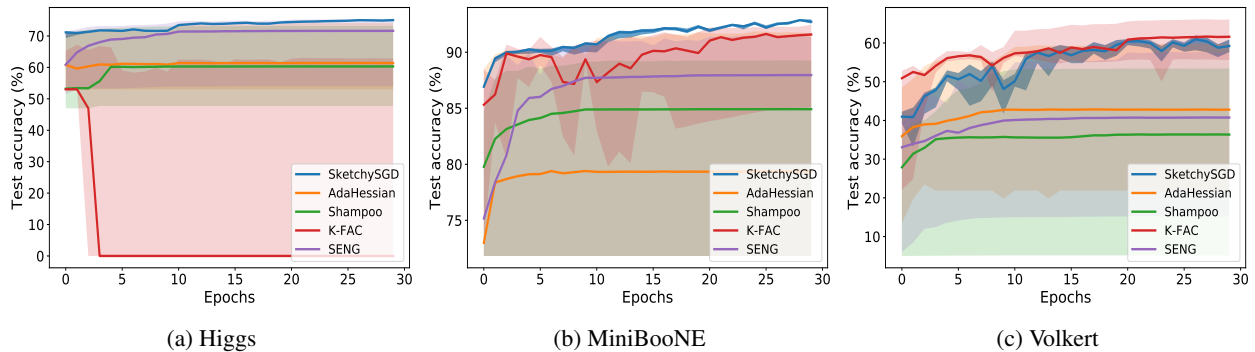


Figure 4: SketchySGD performs best among quasi-Newton methods in terms of robustness, and matches or outperforms the peak test accuracy achieved by other quasi-Newton methods. The solid line indicates the median of test accuracy among different learning rate settings, and the shaded area represents the 75% quantile interval.

#### 4.2.3 Quasi-Newton methods comparison

Experiments in this section compare SketchySGD with the quasi-Newton methods AdaHessian, Shampoo, K-FAC, and SENG on tabular tasks.

Figure 4 and Table 4 present the results of quasi-Newton methods using the same conventions as in Section 4.2.1. They show SketchySGD performs best among quasi-Newton methods in terms of robustness, and matches or outperforms the peak test accuracy achieved by other quasi-Newton methods. Table 5 provides the average per-epoch time of quasi-Newton methods on each tabular task, which shows SketchySGD is the second fastest among all quasi-Newton

Table 4: Peak Test Accuracy of Quasi-Newton Methods for Tabular Tasks with 30 Epochs

Accuracy \ Method	SketchySGD	AdaHessian	Shampoo	K-FAC	SENG
Higgs (%)	75.21	75.07	73.73	72.32	75.33
MiniBooNE (%)	92.99	92.59	89.57	92.67	91.70
Volkert (%)	62.05	64.21	54.56	67.36	58.75

Table 5: Average Per-epoch Time of Quasi-Newton Methods for Tabular Tasks

Time \ Method	SketchySGD	AdaHessian	Shampoo	K-FAC	SENG
Higgs (s)	16.61	39.90	82.46	31.81	14.40
MiniBooNE (s)	2.31	15.56	26.35	10.58	1.88
Volkert (s)	1.32	13.23	46.20	8.66	1.01

methods. While K-FAC sometimes outperforms SketchySGD on the Volkert dataset, it is unreliable: for example, it performs the worst of all methods on Higgs and for certain hyperparameter settings it obtains around 40% test accuracy even on Volkert. K-FAC’s per epoch runtime is also much slower than SketchySGD. Although SENG is slightly faster than SketchySGD, it has poor robustness and peak test accuracy.

## 5 Conclusion

In this paper, we have presented SketchySGD, a fast and robust stochastic quasi-Newton method for machine learning and for deep learning in particular. SketchySGD uses subsampling, randomized low-rank approximation, and dynamic regularization to improve conditioning by approximating the curvature of the loss.

SketchySGD has strong benefits both in theory and in practice. In the convex case, our theory shows that SketchySGD converges to a neighborhood of the optimum at a faster rate than SGD. Our logistic regression experiments validate this claim. In addition, SketchySGD, using a theoretically-motivated learning rate, outperforms SGD, SVRG, and L-BFGS and performs about as well as Adam and SAGA in this setting, even when optimizing the learning rate for SGD, SVRG, and Adam using grid search.

In the non-convex case, SketchySGD converges linearly to the optimum for wide neural networks. Our deep learning experiments show that SketchySGD reliably yields models that generalize well across a variety of learning rates on both tabular and image tasks, while SGD, Adam, and AdamW often fail without extensive hyperparameter tuning. Furthermore, SketchySGD achieves comparable performance to quasi-Newton methods for deep learning, such as AdaHessian, Shampoo, K-FAC, and SENG and runs much faster. Again, SketchySGD is more robust to the learning rate than these quasi-Newton methods.

We believe widespread adoption of SketchySGD will improve the efficiency of large-scale deep learning by reducing the need for hyperparameter tuning. These efficiency gains entail the following benefits: less human effort spent on hyperparameter tuning, a reduction in computational costs, and lower greenhouse gas emissions. Thus, SketchySGD has the potential for a significant positive societal impact that furthers the sustainability goals of green AI.

## A RandPDLowRankApprox

In this section we give the pseudocode for the RandPDLowRankApprox algorithm mentioned in Section 2, which SketchySGD uses to construct the low-rank approximation  $\hat{H}_{S_k}$ .

**Algorithm 2** RandPDLowRankApprox

---

**input:** sketch  $Y$  of  $H_{S_k}$ , test matrix  $\Phi$ , rank  $r_k$

$\nu = \text{eps}(\text{norm}(Y, 2))$  ▷ compute shift

$Y_\nu = Y + \nu\Phi$  ▷ add shift for stability

$C = \text{chol}(\Phi^T Y_\nu)$  ▷ Cholesky decomposition

**if chol fails then** ▷ Hessian is indefinite

  Compute  $[W, \Gamma] = \text{eig}(\Phi^T Y_\nu)$  ▷  $\Phi^T Y_\nu$  is small and square

  Set  $\lambda_k = \lambda_{\min}(\Phi^T Y_\nu)$

$R = W(\Gamma + |\lambda_k|I_k)^{-1/2}W^T$  ▷  $R$  is psd

$B = YR$

$[\hat{V}, \Sigma, \sim] = \text{svd}(B, 0)$  ▷ thin SVD

$\hat{\Lambda} = \max\{0, \Sigma^2 - (\nu + |\lambda_k|)I_k\}$  ▷ remove shift, compute eigs

**return**

$B = Y/C$  ▷ triangular solve

$[\hat{V}, \Sigma, \sim] = \text{svd}(B, 0)$  ▷ thin SVD

$\hat{\Lambda} = \max\{0, \Sigma^2 - \nu I\}$  ▷ remove shift, compute eigs

**output:**  $\hat{V}, \hat{\Lambda}$

---

Algorithm 2 gives the pseudocode.  $\text{eps}(x)$  is defined as the positive distance between  $x$  and the next largest floating point number of the same precision as  $x$ . The test matrix  $\Phi$  is the same test matrix used to generate the sketch  $Y$  of  $H_{S_k}$ . The resulting Nyström approximation  $\hat{H}_{S_k}$  is given by  $\hat{V}\hat{\Lambda}\hat{V}^T$ . In computing  $R$ , the negative square root should be interpreted in the sense of the Moore-Penrose pseudoinverse, so the inverse of a 0 eigenvalue is 0. The resulting Nyström approximation is psd but may have 0 eigenvalues. In our algorithms, this approximation is always used in conjunction with a regularizer to ensure positive definiteness.

Algorithm 2 follows Tropp et al. [2017b], except that it comes with a dynamic-regularization fail-safe step in the case the subsampled Hessian is indefinite and Cholesky fails. Note in the convex case, Cholesky never fails as the subsampled Hessian is always psd. The fail-safe step is useful in the non-convex case where  $H_{S_k}$  may be indefinite, ensuring the resulting Hessian approximation is always psd, so the regularized Hessian approximation is always positive definite and invertible.

## B Controlling minibatch gradient variance

Central to our analysis is the ability to control the variance of a gradient minibatch. A key quantity in this regards is the supremum of the variance of the gradient over the set of minimizers  $\mathcal{W}_*$ :

$$\sigma_*^2 = \sup_{w_* \in \mathcal{W}_*} \frac{1}{n} \sum_{i=1}^n \|g_i(w_*)\|^2.$$

We may view  $\sigma_*^2$  as measure of how well the model fits the training set. Indeed, in the extreme case when the model interpolates the dataset,  $\sigma_*^2 = 0$ . Thus the smaller  $\sigma_*^2$ , the better the model fit. The fact that  $\sigma_*^2$  helps control the variance of minibatch gradient is shown in the following proposition due to [Gower et al., 2021].

**Proposition 9** (Proposition 3.2 [Gower et al., 2021]). *Suppose each  $f_i$  is  $L_i$ -smooth and at least one of the following conditions holds:*

1. Each  $f_i$  is convex
2.  $f$  interpolates the training set.

Suppose the gradient sample  $g_{B_k}$  uses batch-size  $b_g$ . Then for every  $w \in \mathbb{R}^p$ ,

$$\mathbb{E}_{B_k} \|g_{B_k}(w)\|^2 \leq \|g(w)\|^2 + 4\alpha(f(w) - f(w_*)) + 2\sigma^2,$$

where  $\alpha = L_{\max} \frac{n-b_g}{(n-1)b_g}$  and  $\sigma^2 = \frac{1}{b_g} \frac{n-b_g}{n-1} \sigma_*^2$ .

In particular, under interpolation  $\sigma_*^2 = 0$ , so

$$\mathbb{E}_{B_k} \|g_{B_k}(w)\|^2 \leq \|g(w)\|^2 + 4\alpha(f(w) - f(w_*)).$$

Proposition 9 shows that the variance of a minibatch gradient is controlled by the distance to the optimum, the batch-size  $b_g$ , and  $\sigma_\star^2$ . We see that as we increase the batch-size  $b_g$ , the variance of the minibatch gradient decreases. More interestingly, as  $\sigma_\star^2$  decreases the minibatch gradient variance decreases, and the variance vanishes when the model class perfectly fits the data. As items 1. or 2. in Proposition 9 always hold in this paper, we may use this proposition to control the minibatch gradient variance, which is crucial for establishing Theorem 5 and Theorem 19.

## C SketchySGD convergence – convex case

### C.1 Preliminary technical lemmas

Recall the SketchySGD update is given by

$$x_{k+1} = x_k - \eta_k P_k^{-1} g_{B_k},$$

where  $\mathbb{E}_{B_k}[g_{B_k}] = g_k$ . We start by making the following observation about the SketchySGD update.

**Lemma 10** (SketchySGD is SGD in preconditioned space). *At iteration  $k$  define  $f_{P_k}(z) = f(P_k^{-1/2}z)$ , that is define the change of variable  $x = P_k^{-1/2}z$ . Then,*

$$\begin{aligned} g_{P_k}(z) &= P_k^{-1/2} g(P_k^{-1/2}z) \\ H_{P_k}(z) &= P_k^{-1/2} H(x) P_k^{-1/2}. \end{aligned}$$

Hence the SketchySGD update may be realized as

$$\begin{aligned} z_{k+1} &= z_k - \eta_k \bar{g}_{P_k}(z_k) \\ x_{k+1} &= P_k^{-1/2} z_{k+1}, \end{aligned}$$

where  $\bar{g}_{P_k}(z_k) = P_k^{-1/2} g_{B_k}(P_k^{-1/2}z_k)$ .

*Proof.* The first display of equations follow from the definition of the change of variable and the chain rule, while the last display follows from definition of the SketchySGD update and the first display.  $\square$

The preceding lemma shows SketchySGD update may be realized by performing a stochastic gradient step in preconditioned space, and then converting back to the original space. This view will help in establishing the convergence rate of SketchySGD in the convex case.

**Definition 2.** We define  $\sigma_P^2 := \frac{1}{b_g} \frac{n-b_g}{n-1} \sup_{k \geq 0} \frac{1}{n} \sum_{i=1}^n \|P_k^{-1/2} \nabla f_i(w_\star)\|^2$ .

The quantity  $\sigma_P^2$  is the analogue of  $\sigma^2$  from Proposition 9 in preconditioned space.  $\sigma_P^2$  will be a critical quantity in showing convergence of SketchySGD in the convex case.

**Controlling the quality of the preconditioner** In what follows we show that  $\hat{H}_{S_k}^{\rho_k}$  is close to the exact Hessian  $H$  in the Loewner ordering, which shows it makes excellent preconditioner. Below, we state Lemma 12 from Ye et al. [2021] that shows if we sample appropriately then the subsampled Hessian is close to the full Hessian.

**Lemma 11** (Closeness in Loewner ordering between  $H$  and  $H_S$ ). *Let  $H$  be the Hessian of  $f$ ,  $M(w) = \max_{1 \leq i \leq n} \|\nabla^2 f_i(w)\|$  and let  $\xi > 0$  and  $\delta > 0$  be given. Suppose we construct the subsampled Hessian  $H_S$  with  $|S| = O(\frac{M(w)}{\xi} \log(\frac{n}{\delta}))$  samples. Then for  $\zeta_0 = \max\left\{\frac{3\xi+\mu}{3\xi+3\mu}, \frac{1}{2}\right\} \in (0, 1)$  the event*

$$\mathcal{E}^{(1)} = \{(1 - \zeta_0)(H_S + \xi I) \preceq H \preceq (1 + \zeta_0)(H_S + \xi I)\}$$

holds with probability at least  $1 - \delta$ .

Similarly, we may control the approximation quality of the randomized low-rank approximation used in SketchySGD via the following technical result from Zhao et al. [2022].

**Lemma 12** (Controlling low-rank approximation error). *Let  $\tau > 0$  and  $E_k = H_{S_k} - \hat{H}_{S_k}$ . Construct a randomized Nyström approximation from a standard Gaussian random matrix  $\Omega$  with rank  $r_k = O(d_{\text{eff}}(\tau) + \log(\frac{1}{\delta}))$ . Then the event*

$$\mathcal{E}_k^{(2)} = \{\|E_k\| \leq \tau\} \tag{6}$$

holds with probability at least  $1 - \delta$ .

Lemma 12 allows us to establish the following result which shows our low-rank approximation is close to the regularized subsampled Hessian in the Loewner ordering.

**Lemma 13** (Closeness in Loewner ordering between  $H_{S_k}^\xi$  and  $\hat{H}_{S_k}^\xi$ ). *Let  $0 < \zeta < 1$ . Suppose at iteration  $k$  SketchySGD uses a low-rank approximation  $\hat{H}_{S_k}$  to  $H_{S_k}$  with rank  $r_k = O(d_{\text{eff}}(\zeta\xi) + \log(\frac{1}{\delta}))$ . Then with probability at least  $1 - \delta$ ,*

$$(1 - \zeta_0)\hat{H}_{S_k}^\xi \preceq H_{S_k}^\xi \preceq (1 + \zeta_0)(1 + \zeta)\hat{H}_{S_k}^\xi \quad (7)$$

*Proof.* Let  $E_k = H_{S_k} - \hat{H}_{S_k}$ , and note by the properties of the Nyström approximation that  $E_k \succeq 0$  [Tropp et al., 2017b]. Now, notice the event

$$\mathcal{E}_k^{(2)} = \{\|E_k\| \leq \zeta\xi\}$$

holds with probability at least  $1 - \delta$  by Lemma 12. Henceforth, all analysis is conditioned on  $\mathcal{E}_k$ , and therefore the conclusions hold with probability at least  $1 - \delta$ . Now, the regularized Hessian and approximate Hessian satisfy

$$H_{S_k}^\xi = \hat{H}_{S_k}^\xi + E_k, \quad (8)$$

Let  $P = \hat{H}_{S_k}^\xi$ . Then combining (8) with Weyl's inequalities yields

$$\begin{aligned} \lambda_1(P^{-1/2}H_{S_k}^\xi P^{-1/2}) &\leq \lambda_1\left(P^{-1/2}\hat{H}_{S_k}^\xi P^{-1/2}\right) + \lambda_1\left(P^{-1/2}E_k P^{-1/2}\right) \\ &= 1 + \|P^{-1/2}E_k P^{-1/2}\| \leq 1 + \|P^{-1}\|\|E_k\| \leq 1 + \frac{\|E_k\|}{\xi} \leq 1 + \zeta. \end{aligned}$$

To bound the smallest eigenvalue, observe that

$$H_{S_k}^\xi \succeq \hat{H}_{S_k}^\xi \implies H_{S_k}^\xi \succeq P.$$

Thus, conjugating the preceding relation by  $P^{-1/2}$  we obtain

$$P^{-1/2}H_{S_k}^\xi P^{-1/2} \succeq I_p,$$

where  $I_p$  is the  $p \times p$  identity matrix. The preceding inequality immediately yields

$$\lambda_p(P^{-1/2}H_{S_k}^\xi P^{-1/2}) \geq 1.$$

Hence,

$$1 \leq \lambda_p(P^{-1/2}H_{S_k}^\xi P^{-1/2}) \leq \lambda_1(P^{-1/2}H_{S_k}^\xi P^{-1/2}) \leq 1 + \zeta.$$

As an immediate consequence, we obtain the Loewner ordering relation

$$I_p \preceq P^{-1/2}H_{S_k}^\xi P^{-1/2} \preceq (1 + \zeta)I_p$$

which we conjugate by  $P^{1/2}$  to show

$$\hat{H}_{S_k}^\xi \preceq H_{S_k}^\xi \preceq (1 + \zeta)\hat{H}_{S_k}^\xi.$$

The claimed result follows.  $\square$

Combining Lemma 11 and Lemma 13 immediately yields the following corollary. This corollary shows our regularized low-rank approximation is close to the true Hessian and so makes an excellent preconditioner.

**Corollary 2** (Closeness in Loewner ordering between  $H$  and  $\hat{H}^\xi$ ). *Instate the hypotheses of Lemma 11 and Lemma 13 with  $\delta' = \frac{\delta}{2}$ , where  $\delta \in (0, 1)$  is given. Then with probability at least  $1 - \delta$*

$$(1 - \zeta_0)\hat{H}_{S_k}^\xi \preceq H \preceq (1 + \zeta_0)(1 + \zeta)\hat{H}_{S_k}^\xi.$$

Hence

$$1 - \zeta_0 \leq \lambda_p\left(\left(\hat{H}_{S_k}^\xi\right)^{-1/2}H\left(\hat{H}_{S_k}^\xi\right)^{-1/2}\right) \leq \lambda_1\left(\left(\hat{H}_{S_k}^\xi\right)^{-1/2}H\left(\hat{H}_{S_k}^\xi\right)^{-1/2}\right) \leq (1 + \zeta_0)(1 + \zeta).$$

**Corollary 3** (Union bound). *Let  $\mathcal{E} = \bigcap_{k=0}^t \mathcal{E}_k$ , where  $\mathcal{E}_k = \left(\mathcal{E}_k^{(1)} \cap \mathcal{E}_k^{(2)}\right)$  and suppose that at iteration  $k$  we construct  $\hat{H}_{S_k}$  with rank  $r_k = \tilde{O}(d_{\text{eff}}(\zeta\rho_k))$ , where  $\{\rho_k\}$  is the regularization sequence. Then*

$$\mathbb{P}(\mathcal{E}) \geq 1 - \delta.$$

*Proof.* Instating the hypotheses of Lemma 11 and Lemma 13 with  $\delta' = \frac{\delta}{2(t+1)}$ , we obtain for each  $k \in \{0, \dots, t\}$  that

$$\mathbb{P}(\mathcal{E}_k^C) \leq \frac{\delta}{t+1}.$$

Consequently,

$$\mathbb{P}(\mathcal{E}) = 1 - \mathbb{P}(\mathcal{E}^C) \geq 1 - \sum_{k=0}^t \frac{\delta}{t+1} = 1 - \delta.$$

□

**Lemma 14** (Gradient-based suboptimality bound). *Assume the conclusion of Corollary 2 holds. Then*

$$2(1 - \zeta_0)\hat{\mu}(f(w_k) - f(w_\star)) \leq \|P_k^{-1/2}g_k\|^2.$$

*Proof.* Recall  $f_{P_k}(z) = f(P_k^{-1/2}w)$  so Lemma 10 and relative convexity of  $f$  (5) yield

$$\begin{aligned} f_{P_k}(z_\star) &\geq f_{P_k}(z_k) + \langle g_{P_k}(z_k), z_\star - z_k \rangle + \frac{\hat{\mu}}{2} \|z_\star - z_k\|_{H_{P_k}(z_k)}^2 \\ &\geq f_{P_k}(z_k) + \langle g_{P_k}(z_k), z_\star - z_k \rangle + \frac{(1 - \zeta_0)\hat{\mu}}{2} \|z_\star - z_k\|^2 \\ &\geq \min_{z'} \left\{ f_{P_k}(z_k) + \langle g_{P_k}(z_k), z' - z_k \rangle + \frac{(1 - \zeta_0)\hat{\mu}}{2} \|z' - z_k\|^2 \right\} \\ &= f_{P_k}(z_k) - \frac{1}{2(1 - \zeta_0)\hat{\mu}} \|g_{P_k}(z_k)\|^2. \end{aligned}$$

Rearranging, we find

$$2(1 - \zeta_0)\hat{\mu}(f_{P_k}(z_k) - f_{P_k}(z_\star)) \leq \|g_{P_k}(z_k)\|^2.$$

The desired inequality now follows from the preceding display and Lemma 10. □

## C.2 Proof of Theorem 5

Before giving the proof we provide a more detailed statement of Theorem 5, which includes the exact value of  $\eta$ .

**Theorem 15** (SketchySGD convex convergence). *Instate Assumptions 1, 2 and 4. Let  $\zeta_0 = \frac{3\lambda_{r+1}^* + \mu}{3\lambda_{r+1}^* + 3\mu}$ . Run Algorithm 1 with batch sizes  $b_g, b_{h_k} = O\left(\frac{M(w_k)}{\lambda_{r+1}^*} \log\left(\frac{p}{\delta}\right)\right)$ , stepsize  $\eta = \frac{\hat{\mu}}{(1+\zeta)(1+\zeta_0)\bar{L}} \min\left\{\frac{(1-\zeta_0)\epsilon}{2\sigma_P^2}, \frac{(1-\zeta_0)}{(1-\zeta_0)\hat{\mu} + 2\alpha}\right\}$ , fixed regularization  $\rho = \lambda_{r+1}^*$ , and at each iteration constructing the randomized Nyström approximation with rank  $r_k = O(d_{\text{eff}}(\zeta\lambda_{r+1}^*) + \log(\frac{1}{\delta}))$  where  $r > 0$  is fixed. Further, condition on the event  $\mathcal{E} = \cap_{t=1}^T \mathcal{E}_t$ , which holds with probability at least  $1 - \delta$ . Additionally, suppose  $\epsilon \leq \frac{2\sigma_P^2}{\hat{\mu}_P + 2\alpha}$ . Then after  $t \geq (1 + \zeta) \left(2 + \frac{3\lambda_{r+1}^*}{\mu}\right) \frac{\hat{\mu}}{\hat{\mu}} \frac{2\sigma_P^2}{(1-\zeta_0)\hat{\mu}\epsilon} \log\left(\frac{2(f(w_0) - f(w_\star))}{\epsilon}\right)$  iterations,*

$$\mathbb{E}[f(w_t)] - f(w_\star) \leq \epsilon.$$

*Proof.* For convenience in the proof below we define the following quantities:

$$\begin{aligned} P_k &:= \hat{H}_{S_k}^{\lambda_{r+1}^*}, \\ \hat{L}_P &:= (1 + \zeta)(1 + \zeta_0)\hat{L}, \\ \hat{\mu}_P &:= (1 - \zeta_0)\hat{\mu}. \end{aligned}$$

We also observe  $\sigma_P^2$  from Definition 2 is finite as for any  $k$  we have,

$$\frac{1}{n} \sum_{i=1}^n \|P_k^{-1/2} \nabla f_i(w_\star)\|^2 \leq \frac{1}{\lambda_{r+1}^*} \frac{1}{n} \sum_{i=1}^n \|\nabla f_i(w_\star)\|^2.$$

With these preliminaries, we may now begin the proof.

Observe that relative smoothness implies the inequality

$$f(w_{k+1}) \leq f(w_k) - \eta \langle g_k, P_k^{-1} g_{B_k} \rangle + \frac{\eta^2 \hat{L}}{2} \|P_k^{-1} g_{B_k}\|_{H_k}^2.$$

Hence

$$\begin{aligned} f(w_{k+1}) &\leq f(w_k) - \eta \langle g_k, P_k^{-1} g_{B_k} \rangle + \frac{\eta^2 \hat{L}}{2} \|P_k^{-1/2} g_{B_k}\|_{P_k^{-1/2} H_k P_k^{-1/2}}^2 \\ &\stackrel{(i)}{\leq} f(w_k) - \eta \langle g_k, P_k^{-1} g_{B_k} \rangle + \frac{\eta^2 (1 + \zeta_0)(1 + \zeta) \hat{L}}{2} \|P_k^{-1/2} g_{B_k}\|^2 \\ &\stackrel{(ii)}{=} f(w_k) - \eta \langle g_k, P_k^{-1} g_{B_k} \rangle + \frac{\eta^2 \hat{L}_P}{2} \|P_k^{-1/2} g_{B_k}\|^2 \end{aligned}$$

where (i) follows from Corollary 2 whose conclusions hold as we are conditioned on  $\mathcal{E}$ , and (ii) follows from definition of  $\hat{L}_P$ . Next we take the expectation with respect to  $B_k$  to obtain

$$\mathbb{E}_{B_k}[f(w_{k+1})] \leq f(w_k) - \eta \|P_k^{-1/2} g_k\|^2 + \frac{\hat{L}_P \eta^2}{2} \mathbb{E}_{B_k} \left[ \|P_k^{-1/2} g_{B_k}\|^2 \right].$$

We now bound  $\mathbb{E}_{B_k} \left[ \|P_k^{-1/2} g_{B_k}\|^2 \right]$ . By Lemma 10 we have  $\mathbb{E}_{B_k} \left[ \|P_k^{-1/2} g_{B_k}(w_k)\|^2 \right] = \mathbb{E}_{B_k} \left[ \|P_k^{-1/2} g_{B_k}(P_k^{-1/2} z_k)\|^2 \right] = \mathbb{E}_{B_k} \left[ \|\bar{g}_{P_k}(z_k)\|^2 \right]$ . Thus we may apply the expected residual condition (Proposition 9) on the stochastic gradient of the preconditioned objective to conclude

$$\mathbb{E}_{B_k} \left[ \|P_k^{-1/2} g_{B_k}\|^2 \right] \leq \|P_k^{-1/2} g_k\|^2 + 4\alpha(f_{P_k}(z_k) - f_{P_k}(z_*)) + 2\sigma_P^2.$$

Hence

$$\begin{aligned} \mathbb{E}_{B_k}[f(w_{k+1})] &\leq f(w_k) - \eta \|P_k^{-1/2} g_k\|^2 + \frac{\hat{L}_P \eta^2}{2} \left( \|P_k^{-1/2} g_k\|^2 + 4\alpha(f_{P_k}(z_k) - f_{P_k}(z_*)) + 2\sigma_P^2 \right) \\ &= f(w_k) - \eta \left( 1 - \frac{\eta \hat{L}_P}{2} \right) \|P_k^{-1/2} g_k\|^2 + \frac{\hat{L}_P \eta^2}{2} (4\alpha(f(w_k) - f(w_*)) + 2\sigma_P^2), \end{aligned}$$

where in the last equality we have used that  $f_{P_k}(z_k) - f_{P_k}(z_*) = f(w_k) - f(w_*)$  by Lemma 10. As  $\eta \leq 1/\hat{L}_P$ , we see  $1 - \frac{\eta \hat{L}_P}{2} \geq 0$ , so invoking Lemma 14 we obtain

$$\begin{aligned} \mathbb{E}_{B_k}[f(x_{k+1})] &\leq f(w_k) - 2\hat{\mu}_P \eta \left( 1 - \frac{\hat{L}_P \eta}{2} \right) (f(w_k) - f(w_*)) \\ &\quad + \frac{\hat{L}_P \eta^2}{2} (4\alpha(f(w_k) - f(w_*)) + 2\sigma_P^2) \\ &= f(w_k) - \eta \hat{\mu}_P \left( 2 - \hat{L}_P \eta \left( 1 + \frac{2\alpha}{\hat{\mu}_P} \right) \right) (f(w_k) - f(w_*)) + \eta^2 \hat{L}_P \sigma_P^2, \end{aligned}$$

where in the last equality we have gathered like terms. Now as  $\eta = \frac{1}{\hat{L}_P} \min \left\{ \frac{\epsilon \hat{\mu}_P}{2\sigma_P^2}, \frac{\hat{\mu}_P}{\hat{\mu}_P + 2\alpha} \right\}$ , we see

$$2 - \hat{L}_P \eta \left( 1 + \frac{2\alpha}{\hat{\mu}_P} \right) \geq 1.$$

Hence we find (after subtracting  $f(w_*)$  from both sides),

$$\mathbb{E}_{B_k}[f(w_{k+1})] - f(w_*) \leq (1 - \eta \hat{\mu}_P) (f(w_k) - f(w_*)) + \hat{L}_P \eta^2 \sigma_P^2.$$

Now, taking total expectation over all timesteps and recursing yields

$$\mathbb{E}[f(w_t)] - f(w_*) \leq (1 - \eta \hat{\mu}_P)^t (f(w_0) - f(w_*)) + \eta \frac{\hat{L}_P}{\hat{\mu}_P} \sigma_P^2.$$

Using that  $\eta \leq \epsilon \hat{\mu}_P / (2\hat{L}_P \sigma_P^2)$ , the last display simplifies to

$$\mathbb{E}[f(w_t)] - f(w_*) \leq (1 - \eta \hat{\mu}_P)^t (f(w_0) - f(w_*)) + \frac{\epsilon}{2}.$$

From this last display it immediately follows that

$$\mathbb{E}[f(w_t)] - f(w_*) \leq \epsilon$$

after  $t \geq (1 + \zeta) \frac{1 + \zeta_0}{1 - \zeta_0} \frac{\hat{L}}{\hat{\mu}} \max \left\{ \frac{2\sigma_P^2}{(1 - \zeta_0)\hat{\mu}\epsilon}, 1 + \frac{2\alpha}{(1 - \zeta_0)\hat{\mu}} \right\} \log \left( \frac{2(f(w_0) - f(w_*))}{\epsilon} \right)$  iterations. After some algebra we find

$$\frac{1 + \zeta_0}{1 - \zeta_0} = 2 + \frac{3\lambda_{r+1}^*}{\mu}.$$

Furthermore, by our hypothesis on  $\epsilon$  the maximum in the bound on the iteration complexity is attained by the first term.

Thus, after  $t \geq (1 + \zeta) \left( 2 + \frac{3\lambda_{r+1}^*}{\mu} \right) \frac{\hat{L}}{\hat{\mu}} \frac{2\sigma_P^2}{(1 - \zeta_0)\hat{\mu}\epsilon} \log \left( \frac{2(f(w_0) - f(w_*))}{\epsilon} \right)$  iterations

$$\mathbb{E}[f(w_t)] - f(w_*) \leq \epsilon,$$

yielding the complexity statement in the theorem.  $\square$

### C.3 Proof of Corollary 1

We start by stating an abbreviated version of Theorem 4.6 in Gower et al. [2021] for convex functions.

**Theorem 16** (Theorem 4.6 in Gower et al. [2021]). *Let  $f$  be  $L$ -smooth and  $\mu$ -strongly convex and let  $\alpha$  and  $\sigma^2$  be defined as in Proposition 9. Let  $\epsilon > 0$  and suppose we run SGD for  $T$  iterations with step size  $\gamma = \frac{1}{L} \min \left\{ \frac{\mu\epsilon}{2\sigma^2}, \frac{1}{1 + 2\alpha/\mu} \right\}$ . Then*

$$T \geq \frac{L}{\mu} \max \left\{ \frac{2\sigma^2}{\mu\epsilon}, 1 + \frac{2\alpha}{\mu} \right\} \log \left( \frac{2(f(w_0) - f(w_*))}{\epsilon} \right) \implies \mathbb{E}[f(w_T)] - f(w_*) \leq \epsilon.$$

Now we provide the proof of Corollary 1. The idea of the proof is to compare the number of iterations that guarantee SketchySGD and SGD to reach an  $\epsilon$ -suboptimal point in expectation.

*Proof.* From the proof of Theorem 15, for sufficiently small  $\epsilon$ , after

$$(1 + \zeta) \frac{1 + \zeta_0}{1 - \zeta_0} \frac{\hat{L}}{\hat{\mu}} \frac{2\sigma_P^2}{(1 - \zeta_0)\hat{\mu}\epsilon} \log \left( \frac{2(f(w_0) - f(w_*))}{\epsilon} \right) =: T_{\text{SketchySGD}}$$

iterations, SketchySGD is guaranteed to reach an  $\epsilon$ -suboptimal point in expectation. Similarly, Theorem 16 guarantees that for sufficiently small  $\epsilon$ , SGD will reach an  $\epsilon$ -suboptimal point in expectation after

$$\frac{L}{\mu} \frac{2\sigma^2}{\mu\epsilon} \log \left( \frac{2(f(w_0) - f(w_*))}{\epsilon} \right) =: T_{\text{SGD}}$$

iterations. Taking the ratio of  $T_{\text{SGD}}$  to  $T_{\text{SketchySGD}}$ , we find

$$\frac{T_{\text{SGD}}}{T_{\text{SketchySGD}}} = \frac{\sigma^2}{\sigma_P^2} \frac{\kappa}{\hat{\kappa}} \frac{\hat{\mu}}{\mu} \frac{1 - \zeta_0}{1 + \zeta} \left( \frac{3\lambda_{r+1}^*}{\mu} + 2 \right)^{-1},$$

where we used  $\kappa = \frac{L}{\mu}$ ,  $\hat{\kappa} = \frac{\hat{L}}{\hat{\mu}}$ , and  $\frac{1 + \zeta_0}{1 - \zeta_0} = \frac{3\lambda_{r+1}^*}{\mu} + 2$ . Since  $\sigma_P^2 \leq \frac{1}{\lambda_{r+1}^*} \sigma^2$ , we have

$$\frac{T_{\text{SGD}}}{T_{\text{SketchySGD}}} \geq \lambda_{r+1}^* \frac{\kappa}{\hat{\kappa}} \frac{\hat{\mu}}{\mu} \frac{1 - \zeta_0}{1 + \zeta} \left( \frac{3\lambda_{r+1}^*}{\mu} + 2 \right)^{-1}.$$

We now develop a lower bound on the term  $\frac{1 - \zeta_0}{1 + \zeta}$ . Since  $0 < \zeta < 1$ ,  $\frac{1}{1 + \zeta} > \frac{1}{2}$ . In addition,  $1 - \zeta_0 = \frac{2\mu}{3\zeta + 3\mu} > \frac{\mu}{3\lambda_{r+1}^*}$ , since  $\lambda_{r+1}^* \geq \mu$ . Therefore

$$\begin{aligned} \frac{T_{\text{SGD}}}{T_{\text{SketchySGD}}} &\geq \lambda_{r+1}^* \frac{\kappa}{\hat{\kappa}} \frac{\hat{\mu}}{\mu} \frac{\mu}{3\lambda_{r+1}^*} \frac{1}{2} \left( \frac{3\lambda_{r+1}^*}{\mu} + 2 \right)^{-1} \\ &= \frac{\hat{\mu}}{\hat{\kappa}} \frac{\kappa}{6} \left( \frac{3\lambda_{r+1}^*}{\mu} + 2 \right)^{-1}. \end{aligned}$$

Since  $\lambda_{r+1}^* \geq \mu$ ,  $\frac{3\lambda_{r+1}^*}{\mu} + 2 \leq \frac{3\lambda_{r+1}^*}{\mu} + \frac{2\lambda_{r+1}^*}{\mu} = \frac{5\lambda_{r+1}^*}{\mu}$ . Substituting this inequality into the previous display gives

$$\begin{aligned} \frac{T_{\text{SGD}}}{T_{\text{SketchySGD}}} &\geq \frac{\hat{\mu}}{\hat{\kappa}} \frac{\kappa}{6} \left( \frac{5\lambda_{r+1}^*}{\mu} \right)^{-1} \\ &= \frac{\hat{\mu}}{\hat{\kappa}} \frac{L}{30\lambda_{r+1}^*}, \end{aligned}$$

which is the claimed ratio. For least-squares problems,  $\hat{\mu} = \hat{\kappa} = 1$ , implying  $\frac{T_{\text{SGD}}}{T_{\text{SketchySGD}}} \geq \frac{L}{30\lambda_{r+1}^*} = \frac{\lambda_1(H)}{30\lambda_{r+1}(H)}$ .  $\square$

## D Convergence of SketchySGD – non-convex case

### D.1 Relationship between $L$ -smoothness and $\theta$ -PL

Here we show that just as in the case of  $\mu$ -strong convexity where  $\mu \leq L$ , we must have that  $\theta \leq L$ . Thus, for a  $L$ -smooth and  $\theta$ -PL function,  $L/\theta$  may be viewed as the problem condition number.

**Lemma 17.** *A function that is  $L$ -smooth and  $\theta$ -PL always has  $L \geq \theta$ .*

*Proof.* Recall that an  $L$ -smooth function satisfies the inequality (see for instance Theorem 2.1.5 in [Nesterov, 2018])

$$\frac{\|\nabla f(w)\|^2}{2L} \leq f(w) - f(w_*).$$

Thus

$$\|\nabla f(w)\|^2 \leq 2L(f(w) - f(w_)).$$

Now, combining the preceding display with the  $\theta$ -PL condition, we obtain

$$2\theta(f(w) - f(w_*)) \leq \|\nabla f(w)\|^2 \leq 2L(f(w) - f(w_)).$$

Dividing by  $2(f(w) - f(w_*))$  we conclude

$$\theta \leq L.$$

$\square$

### D.2 SketchySGD converges linearly under interpolation and the PL-condition

In this section we show SketchySGD exhibits linear convergence under the hypotheses of interpolation and the  $\theta$ -PL condition. We require the following additional hypothesis,

**Assumption 18.** *The maximum eigenvalue remains of  $\hat{H}_{S_k}^{\rho_k}$  remains bounded throughout the optimization. That is,*

$$\lambda_* = \sup_{k \geq 0} \lambda_{\max}(\hat{H}_{S_k}^{\rho_k}) < \infty.$$

If  $H_{S_k}(w_k)$  were psd for all  $k$ , Assumption 18 would hold trivially by the properties of the Nyström approximation. Indeed, we would have  $\lambda_* \leq L_{\max} + \rho_{\max}$ . Unfortunately, in the non-convex setting the subsampled Hessian need not be psd, which necessitates Assumption 18. The convergence rate here depends on a bound  $\rho_{\min}/\lambda_*$  on the condition number of the approximate Hessian, where  $\rho_{\min}$  lower bounds the minimum eigenvalue.

**Theorem 19** (SketchySGD non-convex convergence). *Instate Assumptions 1, 6, 7, 18. Run SketchySGD from any initialization  $w_0 \in \mathbb{R}^p$  with constant batch sizes  $|B_k| = b_g$  and  $|S_k| = b_h$ , fixed rank  $r$ , regularization sequence  $\{\rho_k\} \in [\rho_{\min}, \rho_{\max}]$ , and fixed step-size  $\eta = \frac{\theta\lambda_*}{(\theta+2\alpha)L}$ . Then the iterate  $w_t$  satisfies*

$$\mathbb{E}[f(w_t)] - f(w_*) \leq \left( 1 - \frac{\theta}{(\theta+2\alpha)} \frac{\rho_{\min}^2}{\lambda_*^2} \frac{\theta}{L} \right)^t (f(w_0) - f(w_)).$$

*Proof.* We start by noting the following bound holds  $\forall k$ ,

$$\rho_{\min} I \preceq \hat{H}_{S_k}^{\rho} \preceq \lambda_* I. \quad (9)$$

Indeed, the lower bound holds by definition of  $\hat{H}_{S_k}^\rho$ , while the upper bound follows by assumption. We now move onto the proof of the main claim. We start by observing that  $L$ -smoothness of  $f$  and the definition of the SketchySGD update (1) imply

$$\begin{aligned} f(w_{k+1}) &\leq f(w_k) + \langle g(w_k), w_{k+1} - w_k \rangle + \frac{L}{2} \|w_{k+1} - w_k\|^2 \\ &= f(w_k) - \eta_k \langle g(w_k), [\hat{H}_{S_k}^\rho]^{-1} g_{B_k}(w_k) \rangle + \frac{L}{2} \eta_k^2 \|[\hat{H}_{S_k}^\rho]^{-1} g_{B_k}(w_k)\|^2. \end{aligned}$$

Now taking expectations with respect to  $B_k$  and using (9) with Cauchy-Schwarz the above display becomes

$$\mathbb{E}_{B_k}[f(w_{k+1})] \leq f(w_k) - \frac{\eta_k}{\lambda_\star} \|g(w_k)\|^2 + \frac{L}{2} \frac{\eta_k^2}{\rho_{\min}^2} \mathbb{E}_{B_k} [\|g_{B_k}(w_k)\|^2].$$

Now, invoking Proposition 9 yields

$$\begin{aligned} \mathbb{E}_{B_k}[f(w_{k+1})] &\leq f(w_k) - \frac{\eta_k}{\lambda_\star} \|g(w_k)\|^2 + \frac{L}{2} \frac{\eta_k^2}{\rho_{\min}^2} \|g(w_k)\|^2 \\ &\quad + 2\alpha L \frac{\eta_k^2}{\rho_{\min}^2} (f(w_k) - f(w_\star)). \end{aligned}$$

We can bound the last term using the  $\theta$ -PL condition, which gives

$$\begin{aligned} \mathbb{E}_{B_k}[f(w_{k+1})] &\leq f(w_k) - \frac{\eta_k}{\lambda_\star} \|g(w_k)\|^2 + \frac{L}{2} \frac{\eta_k^2}{\rho_{\min}^2} \|g(w_k)\|^2 \\ &\quad + \alpha L \frac{\eta_k^2}{\theta \rho_{\min}^2} \|g(w_k)\|^2. \end{aligned}$$

Collecting like terms, we obtain

$$\begin{aligned} \mathbb{E}_{B_k}[f(w_{k+1})] &\leq f(w_k) + \left( -\frac{\eta_k}{\lambda_\star} + \frac{L\eta_k^2}{\rho_{\min}^2} \left( \frac{1}{2} + \frac{\alpha}{\theta} \right) \right) \|g(w_k)\|^2 \\ &= f(w_k) + \left( -\frac{\eta_k}{\lambda_\star} + \frac{L\eta_k^2}{\rho_{\min}^2} \left( \frac{\theta + 2\alpha}{2\theta} \right) \right) \|g(w_k)\|^2. \end{aligned}$$

Setting  $\eta_k = \eta = \frac{\theta \rho_{\min}^2}{(\theta + 2\alpha) \lambda_\star L}$  yields

$$\mathbb{E}_{B_k}[f(w_{k+1})] \leq f(w_k) - \frac{\theta}{(\theta + 2\alpha)} \frac{\rho_{\min}^2 \|g(w_k)\|^2}{2L\lambda_\star^2}.$$

Invoking the  $\theta$ -PL condition again and subtracting off  $f(w_\star)$ , we obtain the bound

$$\mathbb{E}_{B_k}[f(w_{k+1})] - f(w_\star) \leq \left( 1 - \frac{\theta}{(\theta + 2\alpha)} \frac{\rho_{\min}^2 \theta}{\lambda_\star^2 L} \right) (f(w_k) - f(w_\star)).$$

Taking the expectation over all timesteps and applying recursion in the preceding display yields

$$\mathbb{E}[f(w_t)] - f(w_\star) \leq \left( 1 - \frac{\theta}{(\theta + 2\alpha)} \frac{\rho_{\min}^2 \theta}{\lambda_\star^2 L} \right)^t (f(w_0) - f(w_\star)).$$

□

### D.3 Proof of Theorem 8

*Proof.* Let  $\beta' = \frac{\theta}{(\theta + 2\alpha)} \frac{\rho_{\min}^2 \theta}{\lambda_\star^2 L}$ . Theorem 19 shows that if the  $\theta$ -PL condition is satisfied and we run SketchySGD with appropriate step sizes, then the iterates of SketchySGD satisfy

$$\mathbb{E}[f(w_k)] - f(w_\star) \leq (1 - \beta')^k (f(w_0) - f(w_\star)).$$

In the case of a MLP with square-loss, Theorem 4 of Liu et al. [2022] shows the  $\theta$ -PL condition holds in a ball of radius  $R$  about the initialization provided the width of the network at each layer satisfies

$$m^l = \tilde{\Omega} \left( \frac{NR^{6L+2}}{(\lambda_0 - \theta\gamma^{-2})^2} \right).$$

Consequently, to establish the claimed convergence for wide MLPs, we just need to verify for some  $R > 0$  that the iterates  $\{w_k\}_{k \geq 0}$  remain in the ball  $B(w_0, R)$  throughout the optimization with high probability. This verification is straightforward as the algorithm converges linearly.

Let  $\delta > 0$  and set  $R = \frac{\eta\sqrt{2L+4\alpha}}{\rho_{\min}\delta} \frac{f(w_0)}{1-\sqrt{1-\beta^t}}$ . Note that the definition of the radius is not circular even though it depends on  $f(w_0)$ . To see this, observe  $f(w_0) = \|\mathcal{F}_{\text{NN}}(w_0) - y\|^2$  and recall Proposition 1 in Jacot et al. [2018] shows with high probability that for wide NNs  $\|\mathcal{F}_{\text{NN}}(w_0) - y\| = O(1)$ . Hence  $f(w_0) = O(1)$  and is independent of the model, and thus so is  $R$ . We shall show the iterates  $\{w_k\}_{k \geq 0}$  lie in the ball  $B(w_0, R)$  with with probability at least  $1 - \delta$ . To see this, observe that

$$\|w_{k+1} - w_k\| = \eta \left\| \left( \hat{H}_{S_k}^{\rho_k} \right)^{-1} g_{B_k} \right\| \leq \frac{\eta}{\rho_{\min}} \|g_{B_k}\|. \quad (10)$$

Taking the expectation with respect to  $B_k$ , using  $\mathbb{E}\|g_{B_k}\| \leq \sqrt{\mathbb{E}\|g_{B_k}\|^2}$ , and Proposition 9 gives

$$\mathbb{E}_{B_k} \|w_{k+1} - w_k\| \leq \sqrt{\|g(w_k)\|^2 + 4\alpha((f(w_k) - f(w_*)))}.$$

Invoking smoothness of  $f$ , the preceding display becomes

$$\mathbb{E}_{B_k} \|w_{k+1} - w_k\| \leq \frac{\eta}{\rho_{\min}} \sqrt{(2L + 4\alpha)(f(w_k) - f(w_*))}.$$

Now taking the total expectation and using observation (10), we obtain

$$\mathbb{E}\|w_{k+1} - w_k\| \leq \frac{\eta\sqrt{2L+4\alpha}}{\rho_{\min}} \sqrt{\mathbb{E}[f(w_k)] - f(w_*)} \leq \frac{\eta\sqrt{2L+4\alpha}}{\rho_{\min}} (1-\beta^t)^{k/2} (f(w_0) - f(w_*)).$$

Adding up the distance traversed with every step, we find

$$\begin{aligned} \mathbb{E} \left[ \sum_{k=0}^{\infty} \|w_{k+1} - w_k\| \right] &\leq \sum_{k=0}^{\infty} \frac{\eta\sqrt{4\alpha+2L}}{\rho_{\min}} (1-\beta^t)^{k/2} (f(w_0) - f(w_*)) \\ &= \frac{\eta\sqrt{4\alpha+2L}}{\rho_{\min}} \frac{(f(w_0) - f(w_*))}{1-\sqrt{1-\beta^t}} \\ &= \leq \delta R, \end{aligned}$$

where in the last step we used  $f(w_0) - f(w_*) \leq f(w_0)$  as the square-loss is non-negative. Hence by Markov's inequality

$$\mathbb{P} \left( \left\{ \sum_{k=0}^{\infty} \|w_{k+1} - w_k\| \geq R \right\} \right) \leq \delta.$$

Now,

$$w_{k+1} - w_0 = \sum_{j=1}^{k+1} (w_j - w_{j-1}).$$

Thus with probability at least  $1 - \delta$ ,

$$\|w_{k+1} - w_0\| \leq \sum_{j=0}^k \|w_{j+1} - w_j\| \leq \sum_{j=0}^{\infty} \|w_{j+1} - w_j\| \leq R.$$

Consequently, with probability at least  $1 - \delta$ , the optimization trajectory  $\{w_k\}_{k \geq 0}$  remains in the ball  $B(w_0, R)$ .  $\square$

## E Experimental Details

Here we provide more details regarding the logistic regression and deep learning experiments.

Table 6: Dimensions of Logistic Regression Datasets

Dataset	$n_{tr}$	$n_{test}$	$d$
IJCNN	49990	91701	800
News20	15999	3997	1355191
RCV1	20242	677399	47236

**Logistic regression** We compare SketchySGD against SGD, SVRG, Adam, SAGA, and L-BFGS. For SGD, SVRG, and Adam we use a learning rate grid of  $[10^{-3}, 2.5 \cdot 10^{-3}, 5 \cdot 10^{-3}, 10^{-2}, 2.5 \cdot 10^{-2}, 5 \cdot 10^{-2}, 10^{-1}, 2.5 \cdot 10^{-1}, 5 \cdot 10^{-1}, 10^0]$ . The learning rate for SAGA and L-BFGS is automatically selected by scikit-learn. For SketchySGD, we set the learning rate equal to  $1/(1 + 100\lambda_r)$ . In SVRG, we use  $m = \#$  of minibatches (i.e. we update the "snapshot" once every epoch). In Adam, we use the default hyperparameters  $\beta_1 = 0.9$  and  $\beta_2 = 0.999$ . We train for 20 epochs, and use a batch size of 256.

The logistic regression experiments are run on the datasets described in the main text. For News20, we use a random 80-20 split to form a training and test set. For IJCNN, we use a random features transformation that gives us 800 features in total. In Table 6, we provide the dimensions of the datasets, where  $n_{tr}$  is the number of training samples,  $n_{test}$  is the number of testing samples, and  $d$  is the number of features.

**Deep learning on tabular data** We compare SketchySGD against SGD and Adam. All three methods are used to train MLPs. For all three methods, we use a learning rate grid of  $[10^{-4}, 3 \cdot 10^{-4}, 10^{-3}, 3 \cdot 10^{-3}, 10^{-2}, 3 \cdot 10^{-2}, 10^{-1}, 3 \cdot 10^{-1}, 10^0, 3 \cdot 10^0]$ . For all three optimizers, we use weight decay =  $5 \cdot 10^{-4}$ . In Adam, we use the default hyperparameters  $\beta_1 = 0.9$  and  $\beta_2 = 0.999$ . We train for 50 epochs, decaying the learning rate by a factor of 10 at 10 and 20 epochs, and use a batch size of 128. We run SketchySGD with regularization  $\rho = \eta$  that decays with the learning rate, and use rank  $r = 100$  for all the tasks. We also update the Hessian approximation  $\hat{H}$  every two epochs.

Table 7: Dimensions of Tabular Datasets

Dataset \ Size	$n_{tr}$	$n_{test}$	$d$	Network architecture
Higgs	800000	200000	28	[28, 64, 64, 64, 2]
MiniBooNE	104051	26013	50	[50, 128, 128, 128, 2]
Volkert	46648	11662	180	[180, 256, 256, 256, 10]

The tabular data experiments are run on the datasets described in the main text. For all three datasets, we use a random 80-20 split to form a training and test set. In Table 7, we provide the dimensions of the datasets and the network architectures used in training. In Figure 5, we show peak test accuracies across learning rates for all three datasets.

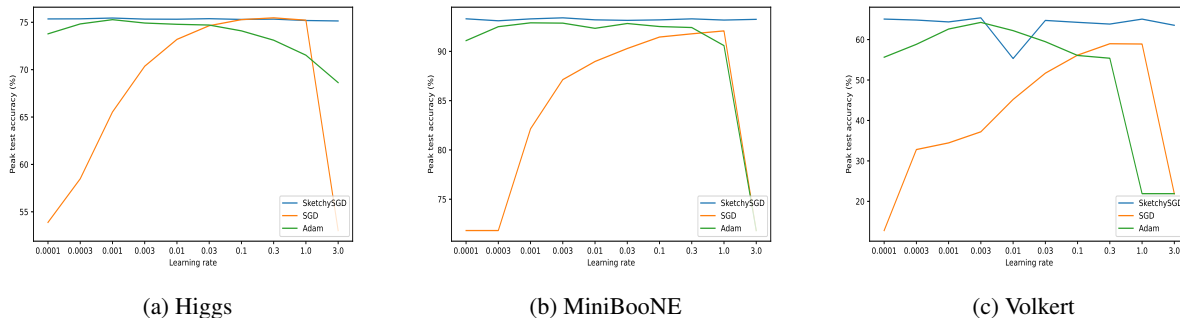


Figure 5: For tabular data, the peak test accuracy produced by SketchySGD does not vary significantly with the learning rate. However, the peak test accuracy produced by SGD and Adam is sensitive to the learning rate.

**Deep learning on image classification** We compare SketchySGD against SGD, Adam, and AdamW. We train ResNet20 on CIFAR10 and ResNet32 on SVHN. We use the train-test splits for CIFAR10 and SVHN that are provided by PyTorch. For all four optimizers, we use a learning rate grid of  $[10^{-4}, 3 \cdot 10^{-4}, 10^{-3}, 3 \cdot 10^{-3}, 10^{-2}, 3 \cdot 10^{-2}, 10^{-1}, 3 \cdot 10^{-1}, 10^0, 3 \cdot 10^0]$ . For all four optimizers, we use weight decay =  $5 \cdot 10^{-4}$ . In Adam and AdamW, we use the default

hyperparameters  $\beta_1 = 0.9$  and  $\beta_2 = 0.999$ . We train for 200 epochs, decaying the learning rate by a factor of 10 at 80, 120, and 160 epochs, and use a batch size of 128. We run SketchySGD with regularization  $\rho = \eta$  that decays with the learning rate, and use rank  $r = 100$  for all the tasks. We also update the Hessian approximation  $\hat{H}$  every two epochs. In Figure 6, we show peak test accuracies across learning rates for both CIFAR10 and SVHN.

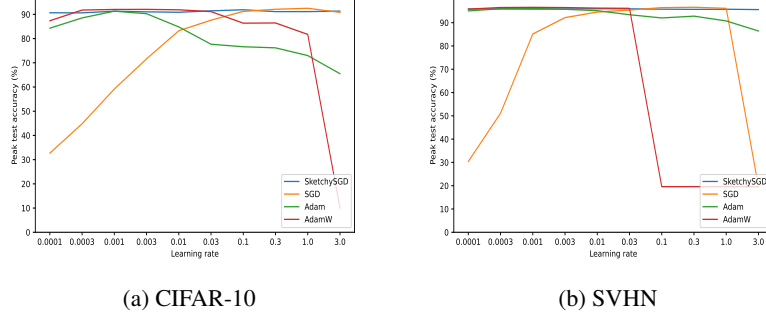


Figure 6: For image classification, the peak test accuracy produced by SketchySGD does not vary significantly with the learning rate. However, the peak test accuracy produced by SGD, Adam, and AdamW is sensitive to the learning rate.

**Deep learning: comparing quasi-Newton methods** We compare SketchySGD against AdaHessian, Shampoo, K-FAC, and SENG. For all five methods, we use a learning rate grid of  $[10^{-4}, 3 \cdot 10^{-4}, 10^{-3}, 3 \cdot 10^{-3}, 10^{-2}, 3 \cdot 10^{-2}, 10^{-1}, 3 \cdot 10^{-1}, 10^0, 3 \cdot 10^0]$  and weight decay  $= 5 \cdot 10^{-4}$ . For AdaHessian, Shampoo, K-FAC, and SENG, we use all the default hyperparameters provided by the authors except learning rate and weight decay. We run SketchySGD with regularization  $\rho = \eta$  that decays with the learning rate, and use rank  $r = 100$  for all the tasks. We also update the Hessian approximation  $\hat{H}$  every two epochs. All the times provided in Table 5 are evaluated on a NVIDIA GeForce RTX 3090 GPU.

For tabular datasets, Higgs, MiniBooNE, and Volkert, we use the same network structures as shown in Table 7. We train for 30 epochs, decaying the learning rate by a factor of 10 at 10 and 20 epochs, and use a batch size of 128. We provide the peak test accuracies across learning rates for all quasi-Newton methods on three tabular datasets in Figure 7. For image classification on CIFAR-10 dataset, we use ResNet20 model. We train for 80 epochs, decaying the learning rate by a factor of 10 at 30, 50, and 70 epochs, and use a batch size of 128. For CIFAR-10 dataset, Figure 8a shows the robustness of quasi-Newton methods in the same conventions as Figure 4, and Figure 8b shows the peak test accuracies across learning rates for all quasi-Newton methods.

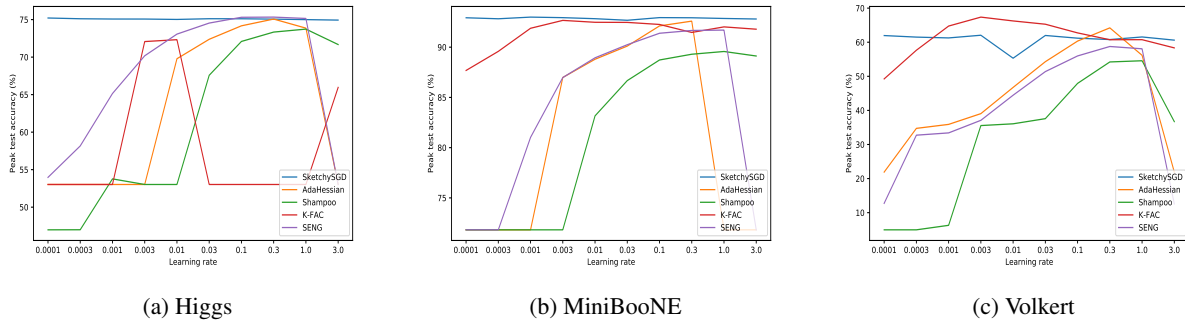


Figure 7: For tabular data, the peak test accuracy produced by SketchySGD does not vary significantly with the learning rate. However, the peak test accuracy produced by other quasi-Newton methods is sensitive to the learning rate.

## F Default Hyperparameters for SketchySGD

In this section we give guidelines for selecting SketchySGD’s hyperparameters.

**Hyperparameters for convex problems** For convex problems, the following hyperparameter settings work well:

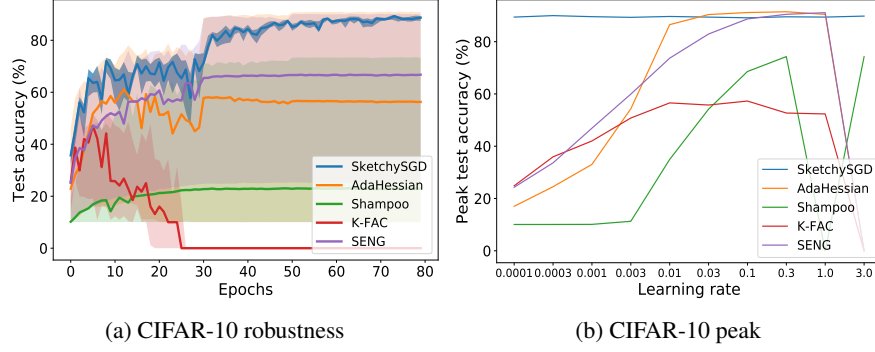


Figure 8: For image classification, SketchySGD performs best among quasi-Newton methods in terms of robustness, and the peak test accuracy produced by SketchySGD does not vary significantly with the learning rate. Only AdaHessian and SENG are capable of producing a comparable test accuracy; however, their performance is less robust to the learning rate and AdaHessian requires full Hessian-vector-product and gradient evaluations.

- Batch sizes set equal  $b_g = b_h$ . We used 256 in this paper.
- Fixed rank  $r = 50$ . This value performed well in all our logistic regression experiments.
- Fixed regularization  $\rho \in \{10^{-1}, 10^{-2}, 10^{-3}\}$  at every iteration. For the logistic regression experiments, we used  $\rho = 10^{-3}$ .
- Learning rate  $\eta = \frac{1}{1+100\hat{\lambda}_r}$ , where  $\hat{\lambda}_r$  is the  $r$ th eigenvalue of the current subsampled Hessian approximation  $\hat{H}$ .
- We recommend computing a fresh approximation  $\hat{H}$  after each epoch or two.

Our learning rate recommendation is motivated by the following theoretical observation. At each iteration we expect to be able to take a step-size on the order of  $L_P^{-1}$ , where  $L_P = \|(\hat{H}_{S_k}^{\rho_k})^{-1/2} H (\hat{H}_{S_k}^{\rho_k})^{-1/2}\|$ . By the triangle inequality and the properties of the Nyström approximation, it is easy to see that

$$L_P \leq 1 + \frac{\|H - H_{S_k}\|}{\rho_k} = 1 + \frac{\|E_{S_k}\|}{\rho_k}.$$

Thus, we expect to be able to take a step-size satisfying

$$\eta = O\left(\frac{1}{1 + \|E_{S_k}\|/\rho_k}\right).$$

Our choice follows by approximating the ratio as  $\|E_{S_k}\|/\rho_k \approx 100\hat{\lambda}_r$ . Empirically we find this choice works well in practice, having used this selection for all the logistic regression experiments.

**Hyperparameters for deep learning** For deep learning we find the following hyperparameter settings work well:

- Batch sizes set equal  $b_g = b_h$ . We used 128 in this paper.
- Fixed rank  $r = 100$ . This value performed well in all our deep learning experiments.
- Fixed learning rate  $\eta = 10^{-2}$ .
- Fixed regularization  $\rho = \eta$  at every iteration.
- We recommend computing a fresh approximation  $\hat{H}$  after each epoch or two. Our experiments compute a new approximation every two epochs.

## References

- Damek Davis, Dmitriy Drusvyatskiy, Sham Kakade, and Jason D Lee. Stochastic subgradient method converges on tame functions. *Foundations of Computational Mathematics*, 20(1):119–154, 2020.
- John Duchi, Elad Hazan, and Yoram Singer. Adaptive subgradient methods for online learning and stochastic optimization. *Journal of Machine Learning Research*, 12(7), 2011.

- Rie Johnson and Tong Zhang. Accelerating stochastic gradient descent using predictive variance reduction. *Advances in Neural Information Processing Systems*, 26, 2013.
- Diederik P Kingma and Jimmy Ba. Adam: A method for stochastic optimization. *arXiv preprint arXiv:1412.6980*, 2014.
- Ruoyu Sun. Optimization for deep learning: theory and algorithms. *arXiv preprint arXiv:1912.08957*, 2019.
- Zhewei Yao, Amir Gholami, Sheng Shen, Mustafa Mustafa, Kurt Keutzer, and Michael Mahoney. AdaHessian: An adaptive second order optimizer for machine learning. In *Proceedings of the AAAI Conference on Artificial Intelligence*, volume 35, pages 10665–10673, 2021.
- Roy Schwartz, Jesse Dodge, Noah A Smith, and Oren Etzioni. Green AI. *Communications of the ACM*, 63(12):54–63, 2020.
- Jorge Nocedal and Stephen J Wright. *Numerical optimization*. Springer, 1999.
- Stephen P Boyd and Lieven Vandenberghe. *Convex optimization*. Cambridge University Press, 2004.
- Yann N Dauphin, Razvan Pascanu, Caglar Gulcehre, Kyunghyun Cho, Surya Ganguli, and Yoshua Bengio. Identifying and attacking the saddle point problem in high-dimensional non-convex optimization. *Advances in neural information processing systems*, 27, 2014.
- Kenneth Levenberg. A method for the solution of certain non-linear problems in least squares. *Quarterly of Applied Mathematics*, 2(2):164–168, 1944.
- Donald W Marquardt. An algorithm for least-squares estimation of nonlinear parameters. *Journal of the Society for Industrial and Applied Mathematics*, 11(2):431–441, 1963.
- Behrooz Ghorbani, Shankar Krishnan, and Ying Xiao. An investigation into neural net optimization via Hessian eigenvalue density. In *International Conference on Machine Learning*, pages 2232–2241. PMLR, 2019.
- Zhewei Yao, Amir Gholami, Kurt Keutzer, and Michael W Mahoney. PyHessian: Neural networks through the lens of the Hessian. In *2020 IEEE international conference on big data (Big data)*, pages 581–590. IEEE, 2020.
- Barak A Pearlmutter. Fast exact multiplication by the Hessian. *Neural Computation*, 6(1):147–160, 1994.
- David P Woodruff. Sketching as a tool for numerical linear algebra. *Foundations and Trends® in Theoretical Computer Science*, 10(1–2):1–157, 2014.
- Per-Gunnar Martinsson and Joel A Tropp. Randomized numerical linear algebra: Foundations and algorithms. *Acta Numerica*, 29:403–572, 2020.
- Nathan Halko, Per-Gunnar Martinsson, and Joel A Tropp. Finding structure with randomness: Probabilistic algorithms for constructing approximate matrix decompositions. *SIAM Review*, 53(2):217–288, 2011.
- Michael B Cohen, Sam Elder, Cameron Musco, Christopher Musco, and Madalina Persu. Dimensionality reduction for k-means clustering and low rank approximation. In *Proceedings of the Forty-seventh Annual ACM Symposium on Theory of Computing*, pages 163–172, 2015.
- Joel A Tropp, Alp Yurtsever, Madeleine Udell, and Volkan Cevher. Practical sketching algorithms for low-rank matrix approximation. *SIAM Journal on Matrix Analysis and Applications*, 38(4):1454–1485, 2017a.
- Joel A Tropp, Alp Yurtsever, Madeleine Udell, and Volkan Cevher. Fixed-rank approximation of a positive-semidefinite matrix from streaming data. *Advances in Neural Information Processing Systems*, 30, 2017b.
- Nicholas J Higham. *Accuracy and stability of numerical algorithms*. SIAM, 2002.
- Charles George Broyden. The convergence of a class of double-rank minimization algorithms 1. general considerations. *IMA Journal of Applied Mathematics*, 6(1):76–90, 1970.
- Dong C Liu and Jorge Nocedal. On the limited memory BFGS method for large scale optimization. *Mathematical Programming*, 45(1):503–528, 1989.
- Ron S Dembo, Stanley C Eisenstat, and Trond Steihaug. Inexact Newton methods. *SIAM Journal on Numerical Analysis*, 19(2):400–408, 1982.
- Richard H Byrd, Gillian M Chin, Will Neveitt, and Jorge Nocedal. On the use of stochastic Hessian information in optimization methods for machine learning. *SIAM Journal on Optimization*, 21(3):977–995, 2011.
- Murat A Erdogdu and Andrea Montanari. Convergence rates of sub-sampled Newton methods. *Advances in Neural Information Processing Systems*, 28, 2015.
- Mert Pilanci and Martin J Wainwright. Newton sketch: A near linear-time optimization algorithm with linear-quadratic convergence. *SIAM Journal on Optimization*, 27(1):205–245, 2017.

- Robert Gower, Dmitry Kovalev, Felix Lieder, and Peter Richtárik. RSN: Randomized subspace Newton. *Advances in Neural Information Processing Systems*, 32, 2019.
- Farbod Roosta-Khorasani and Michael W Mahoney. Sub-sampled Newton methods. *Mathematical Programming*, 174(1):293–326, 2019.
- Raghu Bollapragada, Richard H Byrd, and Jorge Nocedal. Exact and inexact subsampled Newton methods for optimization. *IMA Journal of Numerical Analysis*, 39(2):545–578, 2019.
- Si Yi Meng, Sharan Vaswani, Issam Hadj Laradji, Mark Schmidt, and Simon Lacoste-Julien. Fast and furious convergence: Stochastic second order methods under interpolation. In *International Conference on Artificial Intelligence and Statistics*, pages 1375–1386. PMLR, 2020.
- Roger Grosse and James Martens. A Kronecker-factored approximate Fisher matrix for convolution layers. In *International Conference on Machine Learning*, pages 573–582. PMLR, 2016.
- Minghan Yang, Dong Xu, Zaiwen Wen, Mengyun Chen, and Pengxiang Xu. Sketchy empirical natural gradient methods for deep learning. *arXiv preprint arXiv:2006.05924*, 2020.
- Nicolas Roux, Pierre-Antoine Manzagol, and Yoshua Bengio. Topmoumoute online natural gradient algorithm. *Advances in Neural Information Processing Systems*, 20, 2007.
- Minghan Yang, Dong Xu, Qiwen Cui, Zaiwen Wen, and Pengxiang Xu. NG+: A multi-step matrix-product natural gradient method for deep learning. *arXiv preprint arXiv:2106.07454*, 2021a.
- Vineet Gupta, Tomer Koren, and Yoram Singer. Shampoo: Preconditioned stochastic tensor optimization. In *International Conference on Machine Learning*, pages 1842–1850. PMLR, 2018.
- Donald Goldfarb, Yi Ren, and Achraf Bahamou. Practical quasi-Newton methods for training deep neural networks. *Advances in Neural Information Processing Systems*, 33:2386–2396, 2020.
- Minghan Yang, Dong Xu, Hongyu Chen, Zaiwen Wen, and Mengyun Chen. Enhance curvature information by structured stochastic quasi-Newton methods. In *Proceedings of the IEEE/CVF Conference on Computer Vision and Pattern Recognition*, pages 10654–10663, 2021b.
- Shipu Zhao, Zachary Frangella, and Madeleine Udell. NysADMM: faster composite convex optimization via low-rank approximation. *arXiv preprint arXiv:2202.11599*, 2022.
- Michal Dereziński, Feynman T Liang, Zhenyu Liao, and Michael W Mahoney. Precise expressions for random projections: Low-rank approximation and randomized newton. In H. Larochelle, M. Ranzato, R. Hadsell, M.F. Balcan, and H. Lin, editors, *Advances in Neural Information Processing Systems*, volume 33, pages 18272–18283. Curran Associates, Inc., 2020. URL <https://proceedings.neurips.cc/paper/2020/file/d40d35b3063c11244fbf38e9b55074be-Paper.pdf>.
- Robert Gower, Othmane Sebbouh, and Nicolas Loizou. SGD for structured nonconvex functions: Learning rates, minibatching and interpolation. In *International Conference on Artificial Intelligence and Statistics*, pages 1315–1323. PMLR, 2021.
- Sharan Vaswani, Aaron Mishkin, Issam Laradji, Mark Schmidt, Gauthier Gidel, and Simon Lacoste-Julien. Painless stochastic gradient: Interpolation, line-search, and convergence rates. *Advances in Neural Information Processing Systems*, 32, 2019a.
- Chaoyue Liu, Libin Zhu, and Mikhail Belkin. Loss landscapes and optimization in over-parameterized non-linear systems and neural networks. *Applied and Computational Harmonic Analysis*, 2022.
- Sharan Vaswani, Francis Bach, and Mark Schmidt. Fast and faster convergence of SGD for over-parameterized models and an accelerated perceptron. In *The 22nd International Conference on Artificial Intelligence and Statistics*, pages 1195–1204. PMLR, 2019b.
- Siyuan Ma, Raef Bassily, and Mikhail Belkin. The power of interpolation: Understanding the effectiveness of SGD in modern over-parametrized learning. In *International Conference on Machine Learning*, pages 3325–3334. PMLR, 2018.
- Mikhail Belkin. Fit without fear: remarkable mathematical phenomena of deep learning through the prism of interpolation. *Acta Numerica*, 30:203–248, 2021.
- Kevin Scaman, Cédric Malherbe, and Ludovic Dos Santos. Convergence rates of non-convex stochastic gradient descent under a generic Lojasiewicz condition and local smoothness. In *International Conference on Machine Learning*, pages 19310–19327. PMLR, 2022.
- Aaron Defazio, Francis Bach, and Simon Lacoste-Julien. SAGA: A fast incremental gradient method with support for non-strongly convex composite objectives. *Advances in Neural Information Processing Systems*, 27, 2014.

- Ilya Loshchilov and Frank Hutter. Decoupled weight decay regularization. In *International Conference on Learning Representations*, 2019. URL <https://openreview.net/forum?id=Bkg6RiCqY7>.
- Danil Prokhorov. IJCNN 2001 neural network competition.
- Ken Lang. Newsweeder: Learning to filter netnews. In Armand Prieditis and Stuart Russell, editors, *Machine Learning Proceedings 1995*, pages 331–339. Morgan Kaufmann, San Francisco (CA), 1995. ISBN 978-1-55860-377-6. doi:<https://doi.org/10.1016/B978-1-55860-377-6.50048-7>. URL <https://www.sciencedirect.com/science/article/pii/B9781558603776500487>.
- David D. Lewis, Yiming Yang, Tony G. Rose, and Fan Li. RCV1: A new benchmark collection for text categorization research. *J. Mach. Learn. Res.*, 5:361–397, dec 2004. ISSN 1532-4435.
- Ali Rahimi and Benjamin Recht. Random features for large-scale kernel machines. *Advances in Neural Information Processing Systems*, 20, 2007.
- Adam Paszke, Sam Gross, Francisco Massa, Adam Lerer, James Bradbury, Gregory Chanan, Trevor Killeen, Zeming Lin, Natalia Gimelshein, Luca Antiga, Alban Desmaison, Andreas Kopf, Edward Yang, Zachary DeVito, Martin Raison, Alykhan Tejani, Sasank Chilamkurthy, Benoit Steiner, Lu Fang, Junjie Bai, and Soumith Chintala. Pytorch: An imperative style, high-performance deep learning library. In *Advances in Neural Information Processing Systems 32*, pages 8024–8035. 2019.
- P. Baldi, P. Sadowski, and D. Whiteson. Searching for exotic particles in high-energy physics with deep learning. *Nature Communications*, 5(1), July 2014. doi:10.1038/ncomms5308. URL <https://doi.org/10.1038/ncomms5308>.
- OpenML, miniboone. <https://www.openml.org/search?type=data&status=active&id=41150>. Accessed: 2022-10-07.
- OpenML, volkert. <https://www.openml.org/search?type=data&sort=runs&id=41166&status=active>. Accessed: 2022-05-01.
- Alex Krizhevsky, Geoffrey Hinton, et al. Learning multiple layers of features from tiny images. 2009.
- Yuval Netzer, Tao Wang, Adam Coates, Alessandro Bissacco, Bo Wu, and Andrew Y. Ng. Reading digits in natural images with unsupervised feature learning. In *NIPS Workshop on Deep Learning and Unsupervised Feature Learning 2011*, 2011. URL [http://ufldl.stanford.edu/housenumbers/nips2011\\_housenumbers.pdf](http://ufldl.stanford.edu/housenumbers/nips2011_housenumbers.pdf).
- Kaiming He, Xiangyu Zhang, Shaoqing Ren, and Jian Sun. Deep residual learning for image recognition. In *Proceedings of the IEEE conference on computer vision and pattern recognition*, pages 770–778, 2016.
- Haishan Ye, Luo Luo, and Zhihua Zhang. Approximate Newton methods. *Journal of Machine Learning Research*, 22(66):1–41, 2021. URL <http://jmlr.org/papers/v22/19-870.html>.
- Yurii Nesterov. *Lectures on convex optimization*, volume 137. Springer, 2018.
- Arthur Jacot, Franck Gabriel, and Clément Hongler. Neural Tangent Kernel: Convergence and generalization in neural networks. *Advances in Neural Information Processing Systems*, 31, 2018.